Accommodating LAA within IEEE 802.11ax WiFi Networks for Enhanced Coexistence

Qimei Chen, *Member* and Zhi Ding, *Fellow, IEEE*

***Abstract*—Given the abundance of unlicensed spectrum in 5 GHz band, licensed-assisted-access (LAA) technology presents an efficient and simple approach to alleviate the spectrum crunch in wireless networks. The recent proposal of IEEE 802.11ax as an advanced WiFi standard to accommodate more high rate connections motivates the investigation with respect to the feasibility and benefits of LAA in coexistence with unlicensed user access under this new WiFi protocol. In this paper, we first introduce an enhanced LAA and WiFi coexistence mechanism based on spatial multi-stream transmission within IEEE 802.11ax access. We then derive a stream selection and user replacement strategy based on the proposed synchronous coexistence scheme to improve LAA performance without sacrificing WiFi throughput. We further present a Lyapunov algorithm to optimize the LAA access intensity level with rapid convergence and low-complexity. Numerical results demonstrate the effectiveness of the proposed algorithms, and the mutual benefits of the proposed coexistence framework to both LAA and WiFi users.**

***Index Terms*—LAA, IEEE 802.11ax, coexistence, multi-stream, spatial-reuse, unlicensed spectrum, Lyapunov function.**

I. Introduction

There has been a new wave of excitement generated by launching of the fifth generation (5G) new radio (NR) cellular standard by 3GPP in 2018. This 5G (NR) and other compatible wireless networks must support a diverse range of services ranging from eMBB (enhanced Mobile Broadband) and mMTC (massive Machine Type Communications) to URLLC (Ultra Reliable Low Latency Communications). The future wireless nodes may include a massive number of low latency and high rate devices, and various internet of things (IoT) applications. The skyrocketing demand of bandwidth resources to satisfy these diverse service objectives will further strain the limited licensed spectrum and continue to drive the utility of any residual capacity available in unlicensed spectrum, such as 2.4 GHz and 5 GHz bands. The natural extension of the preliminary development of LTE in unlicensed technology (LTE-U) [1] to NR-based access on unlicensed spectrum (NR-U) makes it possible to achieve a higher degree of control and spectrum efficiency as well as more reliable connections than achieved in basic WiFi networks.

This material is supported by the National Natural Science Foundation Program of China under Grants 61801333 and by the open research fund of National Mobile Communications Research Laboratory, Southeast University under Grant 2019D07.

Q. Chen is with the School of Electronic Information, Wuhan University, Wuhan, China, and also with National Mobile Communications Research Laboratory, Southeast University, Nanjing, 211189, China. e-mail: chenqimei@whu.edu.cn.

Z. Ding is with the Department of Electrical and Computer Engineering, University of California at Davis, Davis, CA 95616, USA. e-mail: zding@ucdavis.edu.

Despite a number of benefits, one of the biggest challenges in the development of LTE-U/NR-U is its coexistence with the widely deployed incumbent IEEE 802.11 networks [2], [3]. Currently, two major coexistence methods for LTE-U are: duty-cycle based carrier-sensing adaptive transmission (CSAT) mechanism proposed by the LTE-U forum to work with the existing 3GPP Releases 10/11/12 [4]–[6], and the listen-before-talk (LBT) licensed-assisted-access (LAA) technology standardized in 3GPP Release 13[1] [7]–[10]. However, both CSAT and LBT rely on vacant periods for unlicensed access, while forbidding co-channel transmissions over unlicensed spectrum by both cellular and WiFi networks. As wireless transceivers for both cellular and WiFi become increasingly sophisticated, innovative coexistence of LAA and WiFi networks are expected to substantially improve the spectrum efficiency and network throughput to serve more users with higher mobility, higher data rate, and lower latency requirements.

Keeping pace with the cellular advances, IEEE 802.11 Working Group also continues to advance WiFi standard technologies. To alleviate the pressure on network capacity by network congestion in density coverage areas, the IEEE 802.11ax amendment is under development and is scheduled for release in 2019 [11]. The major revision in IEEE 802.11ax includes the introduction of orthogonal frequency division multiple access (OFDMA) and the uplink multi-user multiple input multiple output (MU-MIMO) [12], [13]. Similar to their inclusion in 4G/5G cellular technologies, both OFDMA and MU-MIMO can boost spectrum efficiency beyond the traditional WiFi access that relies on CSMA. Their incorporation into IEEE 802.11ax may substantially improve the WiFi network efficiency such that the traditional LAA no longer offers much benefits. Although IEEE 802.11ax is expected to transform future WiFi, there have only been limited efforts devoted to investigating LAA within IEEE 802.11ax WiFi framework. The authors of [14] studies the coexistence issue of traditional LAA with IEEE 802.11ax WiFi, however, there was no consideration of the cooperation issue between these two networks.

To consider the effect of IEEE 802.11ax and fully exploit the potential benefits of LAA, this work will investigate an enhanced coexistence framework and study the resource sharing issue. Leveraging our previous work [15], we will integrate both LAA and WiFi host-nodes into one entity, named hybrid access point (HAP), that is typically equipped with multiple antennas. Different from [15], here we aim to embed LAA transmission into the IEEE 802.11ax protocol.

[1]Without loss of generality, we utilize LAA to denote LTE-U or NR-U technology.

Since IEEE 802.11ax supported both downlink and uplink MU-MIMO, we consider a LAA concept based on spatial reuse [16] with which a subset of the MU-MIMO streams is allocated for LAA transmission, while the remaining streams can be allocated for WiFi transmission. Thereafter, the LAA and WiFi host-nodes would control their assigned streams separately.

In this work, we investigate the compatibility and coexistence of LAA in IEEE 802.11ax WiFi networks. We propose a new networking framework based on an HAP to improve the performance of LAA without degrading WiFi throughput. Specifically, the LAA and WiFi host-nodes would first estimate the signal-to-interference-plus-noise ratio (SINR) information to the LAA and WiFi users, respectively. Based on these information, the HAP would determine the stream selection and user replacement strategy. Thereafter, the HAP reassigned streams to LAA and WiFi users by terminating a subset of WiFi connections and replacing a subset of LAA users. Finally, both LAA and WiFi host-nodes start to transmit separately. To maximize the unlicensed resource utility and to maintain certain level of WiFi performance, we should select the streams with poorer WiFi quality for termination and replace them with LAA users or streams with better (higher) connection quality. This work adopts a select-and-replace algorithm for MU-MIMO downlink transmission with zero-forcing beamforming (ZFBF), which can be optimized with low computation complexity [18]. When the HAP determines the stream reassignment strategy, it would reserve the decision for a transmission opportunity (TXOP) duration. Due to the spatiotemporally varying network environment, we design a Lyapunov algorithm for optimizing the TXOP duration in real time [19]. Our results show that the Lyapunov optimization algorithm leads to fast convergence, low computational complexity, and robustness to non-ergodic systems [20].

To summarize, the major contributions of this paper are as follows.

- We propose a novel LAA structure based on spatial multi-stream transmission within the IEEE 802.11ax WiFi protocol[2]. Taking advantage of the spatial diversity and reuse offered by MU-MIMO, our framework allows co-channel transmissions of LAA and WiFi users over unlicensed spectrum for spectrum efficiency improvement.
- We propose an enhanced LAA and WiFi coexistence framework to improve the unlicensed spectrum utility without degrading WiFi performance. Furthermore, we develop a select-and-replace strategy to achieve spectrum efficiency with low complexity.
- We introduce a Lyapunov algorithm to optimize LAA access duration with demonstrated fast convergence and low complexity. Our performance analyses show the proposed algorithm to achieve asymptotically optimal performance.

We organize the rest of this paper as follows. In Section II, we review several related works and present the motivation of our studies. In Section III, we introduce an enhanced LAA and WiFi coexistence mechanism under a novel LAA structure and describe the system model. Section IV proposes a stream selection and user replacement strategy for the proposed LAA and WiFi coexistence framework before Section V introduces a Lyapunov optimization algorithm for LAA access duration. Section VI provides corroborating numerical results and Section VII concludes the paper.

[2]Note that the basic concepts of this work do apply generally to IEEE 802.11ac as well.

II. Background

A. Related Works

Recognizing the potential of elastic WiFi occupancy, a number of recent works have investigated the coexistence of LAA and WiFi networks. Applying a schedule-based channel access, the authors of [4]–[6] suggested several duty-cycle LAA and WiFi coexistence mechanisms by controlling LAA users to occupy the "on" period and reserve the remaining "off" period for WiFi users. Alternatively, the authors of [7], [8] proposed LBT based coexistence mechanisms for fairness, by defining a sensing-backoff function similar to the CSMA/CA mechanism in IEEE 802.11. Additionally, the authors of [9] considered a full-duplex WiFi access point and suggested a joint mode/rate adaptation strategies for LAA and WiFi coexistence by utilizing self-interference-cancellation. The authors of [10] considered the bursty nature of machine-type communication traffics and developed a coexisting scheme based on a harmonizing-frame. To develop practical coexistence mechanisms, the authors of [15], [17], and [21] utilized the point coordination function and hybrid coordination function (PCF and HCF) together with a CTS-to-Self frame that are inherent to IEEE 802.11 access to embed LAA transmissions within generic IEEE 802.11 networks without retrofitting WiFi access protocol.

Most existing works including the aforementioned proposals for LAA and WiFi coexistence do not allow co-channel signal transmissions more than one wireless user terminals. They do not take advantage of the spatial diversity owing to the multiple antennas that are commonly available on access points and increasingly on individual users. Taking advantage of the spatial diversity, a HAP can leverage MIMO technologies for more dynamic LAA and WiFi coexistence to enhance spatial multi-stream reuse and improve throughput. In [16], the authors proposed to apply massive MIMO in unlicensed band for simultaneous co-channel cellular and WiFi access, while keeping their mutual interference below a regulatory threshold. In [22], the authors also took advantage of the degree of freedom afforded by the multi-antenna base stations for joint LAA and WiFi access. However, both works applied spatial multi-streams for LAA with considering either the performance degradation of WiFi networks or the coordination between LAA and WiFi networks.

In this work, we introduce an enhanced synchronous coexistence mechanism for LAA and WiFi by integrating spatial multi-stream based LAA transmission into the MU-MIMO enabled IEEE 802.11ax protocol to serve both LAA and WiFi networks without conflicts.

B. LAA and IEEE 802.11ax Comparison

We now present a comparative summary of LAA and IEEE 802.11ax protocols. Before the advent of IEEE 802.11ax, there was a consensus that LAA facilitates more efficient use of unlicensed spectrum than the random access of WiFi in heavy or dense coverage scenarios. However, the advanced IEEE 802.11ax improves its efficiency by introducing new physical (PHY) layer and medium access control (MAC) layer specifications including OFDMA and MU-MIMO, which have obscured the distinction between LAA and WiFi. Thus, a natural question arises as to whether LAA technology still offers substantial efficiency benefit in comparison to IEEE 802.11ax.

The comparison of key features between LAA and IEEE 802.11ax are discussed from two perspectives: medium access and resource assignment [11], [23].

- Medium access: In IEEE 802.11ax, WiFi users still compete for access opportunity before receiving channel allocation. WiFi network utilizes CSMA/CA to avoid collision during contention. Specifically, WiFi user performs preamble based carrier sensing to detect other WiFi users with threshold of -82 dBm and energy detection (ED) to detect external interference with threshold of -62 dBm. LAA schemes are usually designed to compete fairly with WiFi users to achieve harmonious coexistence. According to the 3GPP Release 13, LAA users use ED to detect both in and out of network transmissions with threshold of -72 dBm. For this reason, LAA does not demonstrate apparent advantage in medium access.
- Resource assignment: MU-MIMO in both uplink and downlink is supported by IEEE 802.11ax. Thus, LAA in 3GPP and WiFi in IEEE 802.11ax are quite similar in this regard. Moreover, IEEE 802.11ax introduces OFDMA borrowed from 3GPP cellular. Defining a single subcarrier of 78.125 kHz bandwidth to be a tone, IEEE 802.11ax can divide the unlicensed spectrum into multiple resource units (RUs) in OFDMA, and can assign specific RUs to individual users. Under centralized AP control, RU size can respectively equal to 26, 52, 106, 242, 484 or 996 tones within 20 MHz, 40 MHz, 80 MHz, 2×80 MHz, or 1×160 MHz channels. The smallest size of RU has 26 tones, RUs with size larger than 26 can be further divided into smaller RUs. Therefore, bandwidth occupied by a single RU is between 2 MHz to 80 MHz, and the maximum number of RUs in a bandwidth with 20 MHz is 9. An RU with size equal to or larger than 106 tones can also be used for MU-MIMO, which is referred to as a joint MU-MIMO and OFDMA transmission.

In comparison, OFDMA in LAA divides the spectrum into resource blocks (RBs). Each RB in LTE consists of 12 subcarriers, each with bandwidth of 15 kHz and a single time slot duration. Thus, there can be 100 RBs within a 20 MHz bandwidth channel in one time slot. Clearly, the RU in IEEE 802.11ax is much greater than RB. This means that LAA has finer resource allocation granularity to support many more users dynamically than WiFi. Owing to this flexibility, LAA can achieve higher efficiency within IEEE 802.11ax in the frequency domain. However, LAA has less flexibility than IEEE 802.11ax in the time domain, since LAA data transmission in the unlicensed band can only start at the LTE licensed slot boundaries which has a repetition period of 0.5 ms. To better exploit the benefits of LAA, we will introduce an enhanced LAA and WiFi coexistence mechanism based on the IEEE 802.11ax access protocol. Under such coexistence mechanism, the resource waste caused by LAA licensed and unlicensed carriers time synchronization can be ignored compared with the long TXOP duration.

III. Spectrally Efficient Coexistence based on Spatial Reuse

A. A Novel Spatial Reuse based LAA and WiFi Coexistence Mechanism

We introduce an enhanced LAA and WiFi coexistence mechanism based on the MU-MIMO feature of IEEE 802.11ax or IEEE 802.11ac. In this paper, we mainly focus on IEEE 802.11ax with the specific OFDMA feature since it provides higher flexibility in the frequency and spatial domains, protects large multiple uplink and downlink transmissions, and can shorten frame overheads.

First, we describe a wireless access architecture served by an HAP, which was firstly proposed in [15]. The proposed HAP functions simultaneously as a cellular small cell base station (SBS) and a WiFi AP by supporting both LAA and WiFi radio users. The deployment of the HAP permits the jointly coordination of resource management and interference control in both LAA and WiFi networks. The LAA radio of the HAP can access both licensed and unlicensed bands under 3GPP protocol, whereas the WiFi radio of HAP works exclusively in the unlicensed band under IEEE 802.11ax standard.

The proposed HAP has the following benefits. First, deployed by one network service provider, HAP can better manage the mutual interference between the two networks through coordinated frame synchronization and access management of both licensed and unlicensed bands. Secondly, the joint coordinator at HAP can implement more efficient radio resource management strategies by utilizing its channel state information (CSI) knowledge of LAA users. Finally, HAP can control wireless terminals to intelligently access LAA or WiFi for better QoS. It can optimally and flexibly select LAA and WiFi users to associate with the two networks in the unlicensed spectrum.

Based on the HAP and several IEEE 802.11-compliant features, we now propose an enhanced LAA and WiFi coexistence mechanism. Fig. 1(a) presents the flow chart of the proposed LAA and WiFi coexistence procedure, specifically targeting downlink. It consists of two stages: i) stream selection and user replacement; ii) downlink transmission.

1) Downlink Stream Selection and User Replacement: IEEE 802.11ax standard supports MU-MIMO transmission as each AP may utilize up to eight antennas and can generate several beams for data transmission to multiple users simultaneously. To know the CSI of each WiFi user in a MU transmission, the AP should first send a null data packet announcement (NDPA) frame followed by a null data packet

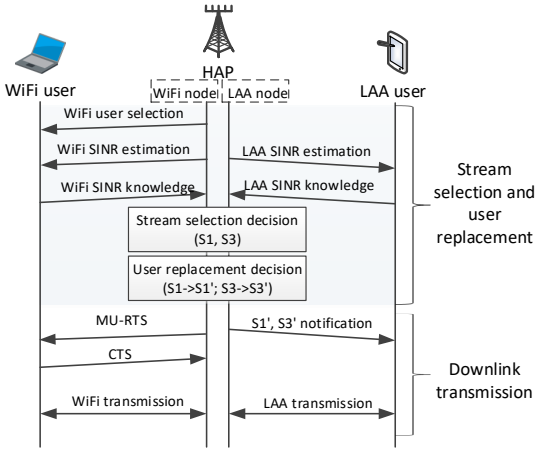

(a) Flow chart of the proposed coexistence procedure.

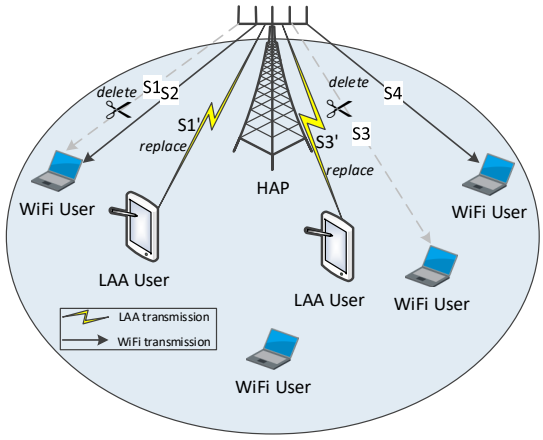

(b) Illustration of stream selection and user replacement.

Fig. 1. WiFi and LAA coexistence mechanism.

(NDP). Then, to solicit the feedback from WiFi users, it transmits a beamforming report (BRP) trigger frame. Thereafter, the WiFi users send their CSI report to the AP [23].

Based on the proposed MU-MIMO process, we develop a stream selection and user replacement strategy with low computational complexity for efficient LAA and WiFi coexistence. Specifically, the HAP first connects with multiple WiFi users synchronously according to the IEEE 802.11ax. Based on the connection, the WiFi element in the HAP estimates the WiFi SINR of each link by sending CSI exchange information to the WiFi users. According to terminal feedbacks, the HAP can select several connections of poorer WiFi data rate to terminate their links, and add association for multiple replacement LAA users. To fully utilize the unlicensed resources freed from the poor WiFi links, the LAA element of the HAP would select a subset of LAA users with better CSI quality to associate. In other words, the HAP would determine the stream allocation between LAA and WiFi networks. Therefore, our proposed coexistence mechanism uses a scheduling technique. Fig. 1(b) illustrates the stream selection and user replacement method.

Note that we can also extend this work to a more general case that replace the terminated WiFi links by LAA or remained WiFi users with better links. Under this circumstance, our goal would turn to improve the spectrum utilization of the coexistence network. However, multiple trigger rounds introduced by all the WiFi users' CSI detection would in turn reduce the spectrum utilization.

2) Joint Downlink Transmission of LAA and WiFi Users: After stream selection and user replacement, the HAP would determine the stream reassignment strategy and this decision would be reserved for a TXOP duration. To implement the LAA downlink, those selected LAA users would reoccupy the vacated streams under the LTE protocol.

For the WiFi downlink, IEEE 802.11ax introduces an MU-RTS/CTS procedure to support MU transmission, as shown in Fig. 2. In order to protect MU transmission, the IEEE 802.11ax AP initiates MU transmission by sending an MU-RTS trigger frame, which includes information about users that would be involved in the upcoming MU downlink and channel allocation. WiFi terminals that decode the MU-RTS frame would reply by transmitting a CTS frame. Thereafter, the WiFi AP would transmit downlink signals to these terminals using MU-MIMO.

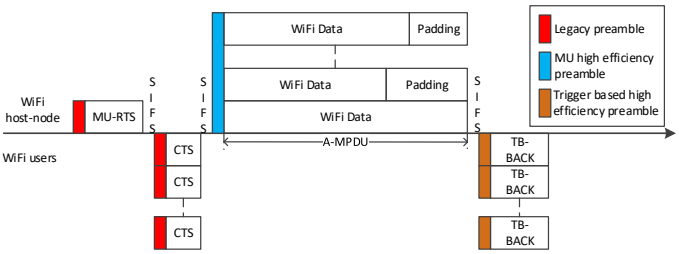

Fig. 2. Downlink multiuser WiFi transmission using OFDMA and MU-MIMO.

On the other hand, the WiFi users that can receive normal WiFi downlink would occupy an entire data portion spanned by RUs of a high efficiency physical layer convergence procedure (PLCP) protocol data unit (PPDU). Each PPDU contains a physical (PHY) header and an aggregated MAC protocol data unit (A-MPDU), as shown in Fig. 4. Data would be transmitted in the A-MPDU. The RU size of OFDMA in a high efficiency multi-user PPDU using OFDMA can be one of the parameters defined earlier. For time synchronization, the start and end of TXOP for LAA transmission should be respectively aligned with the PHY header and ACK of WiFi under the coordination of HAP. LAA or WiFi users with insufficient data will add padding bits to align the time frames. Thereafter, the LAA and WiFi users can send downlink data under 3GPP and IEEE 802.11ax protocols, respectively[3]. After transmission, the WiFi component of the HAP would send a signal to wake up these replaced WiFi users, and then start the next round of stream selection, user replacement, and data transmission processes.

3) The Extension of Joint Uplink Transmission: The process of uplink transmission can be extended by replacing downlink multiuser WiFi transmission (Fig. 2) to uplink multiuser WiFi transmission (Fig. 3). Compared with the downlink

[3]Note that severe interference between WiFi and LAA users may still be likely when the WiFi element transmits preambles and the LAA element transmits data. However, we neglected the effect of such interference since such time period is relatively short and negligible when comparing with the long data transmission duration.

multiuser WiFi transmission, the WiFi host-node in the uplink multiuser WiFi transmission sends a basic trigger before an A-MPDU, which contains the information of involved users and these users' specific information. Therefore, the PHY header would be higher than that in the downlink multiuser WiFi transmission. Moreover, the formulations for downlink data transmission within the A-MPDU should also be changed to the uplink.

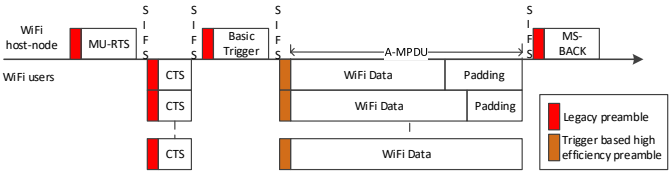

Fig. 3. Uplink multiuser WiFi transmission using OFDMA and MU-MIMO.

In a nutshell, our proposed protocol adopts the scheduling based space division multiple access (SDMA) mechanism while the existing LAA protocol adopts the LBT based time division multiple access (TDMA) mechanism [24]. Specifically, the HAP first connects with multiple WiFi users synchronously according to the IEEE 802.11ax. Based on the CSI of connected WiFi and LAA users, the WiFi users with poor links are replaced with the LAA users with better links. This decision would be reserved for a TXOP duration.

The limitations and tradeoffs of our proposed mechanism are listed as follows. First, the proposed coexistence mechanism is based on IEEE 802.11ax/ac standards. Therefore, it can not be extended to the WiFi protocols with single antenna. Secondly, the proposed coexistence mechanism is based on an HAP. By adopting an HAP the two networks can be jointly controlled and information exchanges across the two networks are made possible. Hence, this mechanism is unsuitable under deployment scenarios where WiFi stations and LAA stations are completely decoupled. It is suitable only in deployment scenarios when an enterprise operates both WiFi and LAA networks in a given area.

B. System Model

We consider a heterogeneous downlink LAA and WiFi MU-MIMO framework based on the concept of HAP, which integrates functionalities of both LTE SBS and WiFi AP into one device unit, as introduced in [15]. In the proposed coexistence mechanism, the WiFi radio of the HAP communicates with WiFi users exclusively in the unlicensed spectrum following the IEEE 802.11ax protocol including MU-MIMO and OFDMA, whereas the SBS radio of the HAP communicates with LAA users in both licensed and unlicensed spectra according to 3GPP cellular protocol.

We assume that the HAP has I antennas such that it can transmit up to I independent downlink streams via spatial multiplexing. With carefully designed linear transmit precoder based on CSI, up to I parallel data streams can arrive orthogonally at I receivers with little or no mutual interference.

For convenience, we use subscript "1" and "0" to denote LAA and WiFi users, respectively, such that $\mathbb{N}_0$ and $\mathbb{N}_1$ denote the WiFi user set and LAA user set, respectively. WiFi and LAA users have only a single antenna. WiFi users communicate by using only the WiFi protocol, whereas LAA users are capable of communicating in either WiFi or LAA mode. We use uppercase boldface letters for matrices and lowercase boldface for vectors. Let $\mathbb{E}[\cdot]$ represent statistical expectation, $(\cdot)^H$ stand for the conjugate transpose, $\mathbf{I}_K$ be an $K \times K$ identity matrix, $|\mathbb{S}|$ denote the cardinality of a user set $\mathbb{S}$, and $\|\mathbf{h}\|$ stand for the Euclidean vector norm, i.e., $\mathbf{h} = \sqrt{\mathbf{h}\mathbf{h}^H}$. Denote $\mathbb{S}/\{s\}$ or $\mathbb{S}/\tilde{\mathbb{S}}$ as removing user s or user set $\tilde{\mathbb{S}}$ from a user set $\mathbb{S}$, respectively. Denote $\mathbb{S} \cup \{s\}$ or $\mathbb{S} \cup \tilde{\mathbb{S}}$ as adding user s or user set $\tilde{\mathbb{S}}$ to a user set $\mathbb{S}$, respectively.

We denote the index set of served users as $\mathbb{M} = \{\omega_1, \omega_2, \cdots, \omega_M\}$, where $\mathbb{M}$ is initially selected from $\mathbb{N}_0$. Note the downlink condition $M \leq I$. Denote the downlink transmit signal vector $\mathbf{x}$ as the selected users' data streams after precoding

$$\mathbf{x} = \sum_{i \in \mathbb{M}} \mathbf{w}(i)\sqrt{p(i)}s(i), \tag{1}$$

where $\mathbf{w}(i) \in \mathbb{C}^{I \times 1}$ is the precoding vector, $p(i)$ is the transmit power scaling factor, and $s(i)$ is the data symbol of user $i \in \mathbb{M}$, respectively. Let the linear channel vector of user i be $\mathbf{h}(i) = [h(i,1), h(i,2), \cdots, h(i,I)] \in \mathbb{C}^{1 \times I}$. Then, its received signal can be written as

$$y(i) = \mathbf{h}(i)\mathbf{x} + z(i), \forall i \in \mathbb{M}, \tag{2}$$

where $z(i) \sim \mathcal{N}(0,1)$ denotes the white Gaussian channel noise.

In this paper, we assume $\mathbf{h}(i)$ to be Rayleigh fading channel with independent identically distributed (i.i.d) zeros mean complex Gaussian entities with unit variance, i.e., $h(i,j) \sim \mathcal{N}(0,1)$, $\forall 0 \leq i \leq M, 0 \leq j \leq I$. We assume that the I data streams have normalized power such that $\mathbb{E}\left[\mathbf{x}\mathbf{x}^H\right] = \mathbf{I}_I$. Furthermore, we consider the case that HAP has full knowledge of the CSI $\mathbf{H} = \left[\mathbf{h}(1)^H, \mathbf{h}(2)^H, \cdots, \mathbf{h}(M)^H\right]^H \in \mathbb{C}^{M \times I}$ for the downlink users. Combining (1) and (2), the received signal at user i is simply

$$y(i) = \mathbf{h}(i)\mathbf{w}(i)\sqrt{p(i)}s(i) + \sum_{j \in \mathbb{M}, j \neq i} \mathbf{h}(i)\mathbf{w}(j)\sqrt{p(j)}s(j) + z(i), \quad \forall i \in \mathbb{M}. \tag{3}$$

In this work, we adopt the ZFBF [25] as the downlink precoder $\mathbf{W} = \mathbf{H}^{\dagger} = \mathbf{H}^H\left(\mathbf{H}\mathbf{H}^H\right)^{-1}$. ZFBF removes the mutual interference among users at the mobile receivers such that $\mathbf{h}(i)\mathbf{w}(j) = \delta(i-j)$. Let $\mathbf{w}(i)$ denote the i-th column of $\mathbf{W}$. As a result, under a sum transmit power P for the HAP, the achievable maximum downlink sum rate respects to the associated users can be formulated as

$$R_{\text{tot}} = \max_{p(i)} \sum_{i \in \mathbb{M}} \log\left(1 + p(i)\right), \quad \text{subject to} \sum_{i \in \mathbb{M}} \gamma^{-1}(i)p(i) \leq P, \tag{4}$$

where $\gamma(i) = \|\mathbf{w}(i)\|^{-2}$ and $\gamma(i)^{-1}p(i)$ is the transmit power allocated to user i. It is well known that the power allocation $p(i)$ can be optimized by water-filling [25]

$$p(i) = \left(\mu\gamma(i) - 1\right)^+, \tag{5}$$

where $(x)^+ = \max\{x, 0\}$, and the water level μ should satisfy

$$\sum_{i \in \mathbb{M}} \left(\mu - \gamma(i)^{-1}\right)^+ = P. \tag{6}$$

IV. Stream Scheduling and User Replacement

We now present a stream scheduling and user replacement strategy for harmonious LAA and WiFi coexistence. From (4)-(6), data rates of the original selected WiFi users, $R_0(m)$, can be formulated as

$$R_0(m) = \log\left[1 + \left(\mu^o \gamma(m) - 1\right)^+\right], \quad \forall m \in \mathbb{M}, \tag{7}$$

where $\gamma(m)$ comes from (6) when all of the streams are associated with the WiFi users, P_0 is the transmission power of the WiFi transmitter in HAP, and

$$\mu^o = M^{-1}\left(P_0 + \sum_{m\in\mathbb{M}} \gamma(m)^{-1}\right). \tag{8}$$

To ensure the performance of WiFi network, the operator will set a minimum rate threshold R_{T} according to its specifical requirement and determine those WiFi users with $R_0(m) \le R_{\mathrm{T}}, \forall m \in \mathbb{M}$ for downlink termination. We can denote the set of terminated WiFi users as $\mathbb{K}$ with cardinality $K = |\mathbb{K}|$.

Having identified $\mathbb{K}$, LAA users can potentially reoccupy these resources. To improve the unlicensed spectrum efficiency, we can select only those LAA users with strong channel gain or $\|\mathbf{h}(\ell)\|$. However, such a simplistic solution based on channel gain does not necessarily lead to the best rate improvement since a newly added user with a large gain may cause substantially high mutual interference with existing terminals.

We now propose a *greedy* selection algorithm by adding the LAA user that can achieve the maximum rate increment. According to (4)-(6), γ is a key parameter in determining the sum rate of the selected user set. To avoid the complexity required to iteratively update γ and the precoder, we introduce an efficient algorithm for finding channel vector $\boldsymbol{v}$ as follows.

1) To initialize, let the initially serviced user set be $\mathbb{M}^{(0)} = \mathbb{M}/\mathbb{K}$ with cardinality $M^{(0)} = \left|\mathbb{M}^{(0)}\right|$, and define $\mathbb{N}_1^{(0)} = \mathbb{N}_1$. Starting from iteration $k = 0$, we shall update the user set $\mathbb{M}^{(k)}$ of cardinality $M^{(k)}$ for $k = 1, 2\cdots$ until all spatial multiplexing diversity has been exhausted. Define

$$\mathbf{H}_{\mathbb{M}^{(k)}} = \left[\mathbf{h}^H(1), \cdots, \mathbf{h}^H(M^{(k)})\right]^H. \tag{9}$$

2) Since ZFBF is a linear precoder that maximizes the output SINR of each stream, the beamforming weight vector in the k-th iteration can be expressed as [26]

$$\mathbf{w}(i) = \left(\frac{\mathbf{h}(i)\mathbf{P}^{\perp}(i)}{\mathbf{h}(i)\mathbf{P}^{\perp}(i)\mathbf{h}^H(i)}\right)^H, \quad \forall i \in \mathbb{M}^{(k)}, \tag{10}$$

where

$$\mathbf{P}^{\perp}(i) = \mathbf{I}_I - \mathbf{H}^H_{\mathbb{M}^{(k)}/\{i\}}\left(\mathbf{H}_{\mathbb{M}^{(k)}/\{i\}}\mathbf{H}^H_{\mathbb{M}^{(k)}/\{i\}}\right)^{-1}\mathbf{H}_{\mathbb{M}^{(k)}/\{i\}}. \tag{11}$$

Here $\mathbf{H}_{\mathbb{M}^{(k)}/\{i\}}$ is a matrix formed by removing the i-th row from $\mathbf{H}_{\mathbb{M}^{(k)}}$ which is the channel matrix of all the selected users in the k-th iteration.
Define $\boldsymbol{v}(i) = \mathbf{h}(i)\mathbf{P}^{\perp}(i)$ as the effective channel vector of user i. We further define the orthogonal components of channel vectors of the remaining LAA users as $\boldsymbol{g}$, which are orthogonal to the space spanned by the channels of the selected users and can be written as

$$\boldsymbol{g}(j) = \mathbf{h}(j)\left\{\mathbf{I}_I - \mathbf{H}^H_{\mathbb{M}^{(k)}}\left(\mathbf{H}_{\mathbb{M}^{(k)}}\mathbf{H}^H_{\mathbb{M}^{(k)}}\right)^{-1}\mathbf{H}_{\mathbb{M}^{(k)}}\right\}, \quad \forall j \in \mathbb{N}_1^{(k)}. \tag{12}$$

Note that both $\boldsymbol{v}(i)$ and $\boldsymbol{g}(j)$ depend on the selected user set in the k-th iteration $\mathbb{M}^{(k)}$.

3) By adding a new LAA user ℓ from $\mathbb{N}_1^{(k)}$ to $\mathbb{M}^{(k)}$, we have updated $\mathbb{N}_1^{(k+1)} = \mathbb{N}_1^{(k)}/\{\ell\}$ and $\mathbb{M}^{(k+1)} = \mathbb{M}^{(k)} \cup \{\ell\}$. Then, the effective channel vector of the newly added LAA user ℓ can be expressed based on the formulation of $\boldsymbol{v}(i)$ and $\boldsymbol{g}(j)$ as [27]

$$\begin{aligned}\boldsymbol{v}_\ell^+(\ell) =& \mathbf{h}(\ell)\left\{\mathbf{I}_I - \mathbf{H}^H_{\mathbb{M}^{(k)}}\left(\mathbf{H}_{\mathbb{M}^{(k)}}\mathbf{H}^H_{\mathbb{M}^{(k)}}\right)^{-1}\mathbf{H}_{\mathbb{M}^{(k)}}\right\}\\ =& \boldsymbol{g}(\ell),\end{aligned} \tag{13}$$

while the updated $\boldsymbol{v}_\ell^+(i)$ of all the already selected users can be derived as

$$\begin{aligned}\boldsymbol{v}_\ell^+(i) =& \mathbf{h}(i)\{\mathbf{I}_I - \\ &\mathbf{H}^H_{\mathbb{M}^{(k+1)}/\{i\}}\left(\mathbf{H}_{\mathbb{M}^{(k+1)}/\{i\}}\mathbf{H}^H_{\mathbb{M}^{(k+1)}/\{i\}}\right)^{-1}\mathbf{H}_{\mathbb{M}^{(k+1)}/\{i\}}\Big\}\\ =& \frac{\gamma(i)\|\boldsymbol{g}(\ell)\|^2}{\gamma(i)\|\boldsymbol{g}(\ell)\|^2 + |\boldsymbol{v}(i)\mathbf{h}^H(\ell)|^2}\left(\boldsymbol{v}(i) - \frac{\boldsymbol{v}(i)\mathbf{h}^H(\ell)}{\|\boldsymbol{g}(\ell)\|^2}\boldsymbol{g}(\ell)\right), \quad \forall i \in \mathbb{M}^{(k)}.\end{aligned} \tag{14}$$

Therefore, the updated $\boldsymbol{v}_\ell^+(i)$ can be generally expressed as

$$\boldsymbol{v}_\ell^+(i) = \begin{cases} \frac{\gamma(i)\|\boldsymbol{g}(\ell)\|^2}{\gamma(i)\|\boldsymbol{g}(\ell)\|^2 + \left|\boldsymbol{v}(i)\mathbf{h}^H(\ell)\right|^2}\left(\boldsymbol{v}(i) - \frac{\boldsymbol{v}(i)\mathbf{h}^H(\ell)}{\|\boldsymbol{g}(\ell)\|^2}\boldsymbol{g}(\ell)\right), & i \ne \ell,\\ \boldsymbol{g}(\ell), & i = \ell. \end{cases} \tag{15}$$

Similarly, since $\boldsymbol{g}(\ell) \perp \boldsymbol{v}(\ell)$, we have

$$\gamma_\ell^+(i) = \left\|\boldsymbol{v}_\ell^+(i)\right\|^2 = \begin{cases} \frac{\gamma^2(i)\|\boldsymbol{g}(\ell)\|^2}{\gamma(i)\|\boldsymbol{g}(\ell)\|^2 + \left|\boldsymbol{v}(i)\mathbf{h}^H(\ell)\right|^2}, & i \ne \ell,\\ \|\boldsymbol{g}(\ell)\|^2, & i = \ell. \end{cases} \tag{16}$$

Thereafter, we can find the updated $\boldsymbol{g}_\ell^+(j)$ with the same method as in $\boldsymbol{v}_\ell^+(i)$, which can be expressed as

$$\boldsymbol{g}_\ell^+(j) = \boldsymbol{g}(j) - \frac{\boldsymbol{g}(j)\boldsymbol{g}^H(\ell)}{\|\boldsymbol{g}(\ell)\|^2}\boldsymbol{g}(\ell). \tag{17}$$

4) The data rates for both LAA and WiFi users can be obtained. Denote the set of added LAA users as $\mathbb{L} = \{\Gamma_1, \Gamma_2, \cdots, \Gamma_L\}$ with cardinality $L = |\mathbb{L}|$. Moreover, we assume P_1 as the transmission power of the LAA components in HAP. Combined with (4)-(6), the data rate of the replaced LAA users, $R_1(\ell)$, and the remaining associated WiFi users, $\tilde{R}_0(n)$, can be respectively expressed as

$$R_1(\ell) = \log\left(1 + \left(\mu\gamma(\ell) - 1\right)^+\right), \quad \forall \ell \in \mathbb{L}, \tag{18}$$

$$\tilde{R}_0(n) = \log\left(1 + \left(\mu\gamma(n) - 1\right)^+\right), \quad \forall n \in \mathbb{M}/\mathbb{K}. \tag{19}$$

Here $\gamma(\ell)$, $\forall \ell \in \mathbb{L}$ and $\gamma(n)$, $\forall n \in \mathbb{M}/\mathbb{K}$ come from the update of (16) when a subset of the streams are

TABLE I
STREAM SCHEDULING AND USER REPLACEMENT STRATEGY.

Algorithm 1 Stream scheduling and user replacement strategy.

Let $\mathbb{M}$ be the set of associated WiFi user group.
Calculate the data rate of WiFi user m, $R_0(m)$, $\forall m \in \mathbb{M}$.
Find the WiFi users with $R_0(m) \leq R_{\mathrm{T}}$, $\forall m \in \mathbb{M}$, and remove them from the user group $\mathbb{M}$.
Update $\mathbb{M}$ and $\mathbf{H}_{\mathbb{M}}$.
Set add_flag$= 1$.
While $M \leq I$ and add_flag$= 1$
    Add an LAA user to maximize data rate increment, i.e., $\ell = \arg\max_{i \in \mathbb{N}_1} R_{\mathrm{tot}}\left(\mathbb{M} \cup \{i\}\right)$.
    Let $\triangle R = R_{\mathrm{tot}}\left(\mathbb{M} \cup \{\ell\}\right) - R_{\mathrm{tot}}\left(\mathbb{M}\right)$.
    If $\triangle R > 0$ and $\tilde{R}_0(n) > R_{\mathrm{T}}, \forall n \in \mathbb{M}/\mathbb{K}$ **then**
        Update $\mathbb{N}_1 = \mathbb{N}_1/\{\ell\}$ and $\mathbb{M} = \mathbb{M} \cup \{\ell\}$.
        Update $\boldsymbol{v}$, γ, and $\boldsymbol{g}$ according to (15), (16), and (17), respectively.
    else
        Set add_flag$= 0$
    End If
End While

associated with the LAA users, while the remaining ones are associated with the WiFi users. Furthermore,

$$\mu = \left[\frac{1}{L}\left(P_1 + \sum_{i \in \mathbb{L}} \frac{1}{\gamma(i)}\right) + \frac{1}{M-K}\left(P_0 + \sum_{j \in \mathbb{M}/\mathbb{K}} \frac{1}{\gamma(j)}\right)\right]. \tag{20}$$

The detailed progress for the stream scheduling and user replacement strategy are listed in Table I. Specifically, the HAP first removes the WiFi users with $R_0(m) \leq R_{\mathrm{T}}, \quad \forall m \in \mathbb{M}$. Next, it adds one LAA user at a time based on CSI measurements by selecting LAA user that can provide the largest data rate increase. From (18) and (19), $R_{\mathrm{tot}} = \sum_{\ell \in \mathbb{L}} R_1(\ell) + \sum_{n \in \mathbb{M}/\mathbb{K}} \tilde{R}_0(n)$. The HAP would stop to add LAA users until it cannot further increase the system data rate or the data rates of existing WiFi users are less than the threshold. Similarly, the addition of inactive WiFi users back to the active set also follows the evaluation of their expected rate feedback, which is possible through regular WiFi random access. In this work, we will refresh the system every TXOP duration.

V. LYAPUNOV BASED TXOP LENGTH OPTIMIZATION

A. Problem Formulation of TXOP Optimization

The determination of the TXOP for LAA access intensity depends on the traffic intensity of WiFi networks. In a WiFi environment with heavy traffic, aggressive LAA access based on a long TXOP duration could cause severe WiFi performance degradation. Conversely, if the TXOP duration is too short, then unlicensed spectrum with a light traffic load would be under utilized. Different from the related work [28] that has discussed TXOP optimization for IEEE 802.11ax, in this section, we consider the optimization of the TXOP duration for LAA networks by reacting to the experience of WiFi users[4]. In addition, we introduce two tradeoff parameters to separately control the LAA and WiFi networks.

First, we assume that both LAA and WiFi components in HAP operate in time slots indexed by $\mathbb{T} = \{0, 1, 2, \cdots\}$. Let $T_0(t)$ and $T_1(t)$ be the WiFi PPDU length with the ACK overhead and the TXOP duration for LAA, respectively, as shown in Fig. 4. Assuming further that the PPDU lengths with the ACK overheads for each WiFi user in different streams are the same, such that $T_0(t) = T_0, \ \forall t \in \mathbb{T}$. For time synchronization, we assume the TXOP length $T_1(t)$ must be an integer multiple of T_0. When an LAA user completes its transmission, it will send padding bits for the remaining duration. Therefore, we derive the relation between $T_1(t)$ and T_0 as follows,

$$T_1(t) = J\left(t\right) T_0, \quad \forall t \in \mathbb{T}. \tag{21}$$

Here $J\left(t\right)$ is an integer, which denotes the number of PPDUs included in an LAA TXOP within time slot t. The maximum PPDU length is 5.484 ms [29].

Denote $Q_0(k,t)$ and $Q_1(\ell,t)$ as the queue length of WiFi user k and LAA user ℓ at time slot t, respectively. Let $A_0(k,t)$ and $A_1(\ell,t)$ be the amount of data entering the downlink queues for WiFi user k and LAA user ℓ at time t, respectively. Then the queue length variation as a result of the downlink rate $R_0(k,t)$ for user k according to (7) can be written as

$$Q_0\left(k, t+1\right) = \left[Q_0\left(k,t\right) - R_0\left(k,t\right)\widetilde{T}_0\right]^+ + A_0(k,t), \quad \forall k \in \mathbb{K}, t \in \mathbb{T}, \tag{22}$$

where $\widetilde{T}_0 = T_0 - T_{\mathrm{overhead}}$ is the duration of WiFi data transmission.

Similarly, the queue length variation for LAA user ℓ due to the downlink rate $R_1\left(\ell,t\right)$ according to (18) can be written as

$$Q_1\left(\ell, t+1\right) = \left[Q_1\left(\ell,t\right) - R_1\left(\ell,t\right)T_1(t)\right]^+ + A_1(\ell,t), \quad \forall \ell \in \mathbb{L}, t \in \mathbb{T}. \tag{23}$$

In this part of the work, our objective is to maximize the throughput of LAA by fully utilizing the unlicensed spectrum while limiting the delay of WiFi users below a threshold. Based on the rate $R_1\left(\ell,t\right)$, maximizing the throughput of LAA network is equivalent to maximizing TXOP for LAA users. Therefore, we can define the performance enhancement of LAA user ℓ in time slot t as

$$H\left(\ell,t\right) = \min\left\{\frac{Q_1\left(\ell,t\right)}{R_1\left(\ell,t\right)}, T_1\left(t\right)\right\}, \quad \forall \ell \in \mathbb{L}, \tag{24}$$

which represents the true transmission duration of each LAA user.

We now formulate the TXOP optimization problem into maximizing the overall true transmission duration of LAA

[4]Different from the LAA specification that TXOP length is limited to 8 ms, in this work, the TXOP duration can be extended longer.

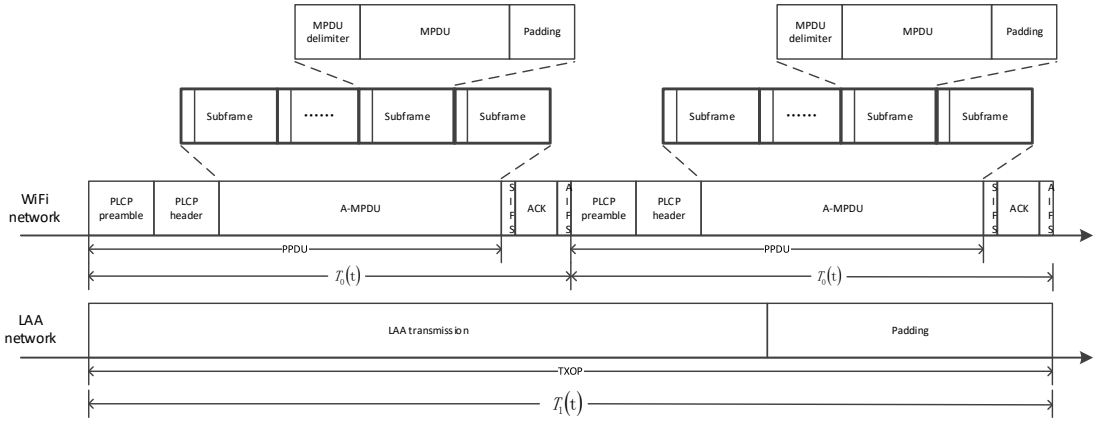

Fig. 4. The relation between the lengths of PPDU and TXOP, which are assigned for WiFi and LAA users respectively.

users by limiting each WiFi user's performance loss.

$$(\mathcal{P}1): \quad \max_{\{J(t)\}} \lim_{T\to\infty} \frac{1}{T}\sum_{t=1}^{T}\mathbb{E}\left[\sum_{\ell=1}^{L} H(\ell,t)\right], \tag{25a}$$

$$\text{subject to} \quad T_1(t) = J(t)\,T_0, \quad \forall t \in \mathbb{T}, \tag{25b}$$

$$\sum_{j=0}^{J(t)-1} Q_0(k,t+j) \le \beta(k), \quad \forall k \in \mathbb{K}, t \in \mathbb{T}, \tag{25c}$$

$$T_1(t) - H(\ell,t) \le \alpha(\ell) < T_0, \quad \forall \ell \in \mathbb{L}, t \in \mathbb{T}, \tag{25d}$$

where $\beta(k)$ denotes the sum delay loss tolerance for WiFi user k in a TXOP length, and $\alpha(\ell)$ represents the maximum padding length for LAA user ℓ required by the time synchronization between the PPDU and TXOP lengths. Constraint (25c) enforces the average delay loss of WiFi network below $\beta(k)$. Constraint (25d) concerns with the unlicensed spectrum utilization when maximizing the overall system throughput.

Clearly, the objective function in $(\mathcal{P}1)$ reflects the long-term average utilization of the unlicensed resources for LAA. The optimization $(\mathcal{P}1)$ is an infinite-horizon Markov decision process (MDP) which can be solved by standard MDP algorithms, such as the linear programming reformulation or value iteration. However, the computational complexity of these traditional solutions can be formidable [19], [20], particularly it is required to solve and store the optimal policies in each step t. Thus, it becomes critical to find an alternative algorithm that approximates the solution to $(\mathcal{P}1)$. In this paper, we propose a Lyapunov based TXOP length optimization algorithm for LAA network to handle $(\mathcal{P}1)$.

We first introduce the concept of a virtual queue such that the queue dynamics with WiFi and LAA users are respectively characterized by X_0 and X_1, which can be given by

$$X_0(k,t+1) = [X_0(k,t) - D_0(k,t)]^+ + C_0(k,t), \forall k \in \mathbb{K}, t \in \mathbb{T}, \tag{26}$$

$$X_1(\ell,t+1) = [X_1(\ell,t) - D_1(\ell,t)]^+ + C_1(\ell,t), \forall \ell \in \mathbb{L}, t \in \mathbb{T}. \tag{27}$$

Here, we have $D_0(k,t) = \sum_{j=0}^{J(t)-1} R_0(k,t+j)\,\widetilde{T}_0$, $C_0(k,t) = \beta(k)$, $D_1(\ell,t) = T_1(t) - H(\ell,t)$, and $C_1(\ell,t) = \alpha(\ell)$. Next, we define the following auxiliary objective

$$(\mathcal{P}2): \quad \max_{\{J(t)\}} \lim_{t\to\infty} \frac{1}{T}\sum_{t=1}^{T}\mathbb{E}\left[\sum_{\ell=1}^{L} H(\ell,t)\right], \tag{28a}$$

$$\text{subject to} \quad T_1(t) = J(t)\,T_0, \quad \forall t \in \mathbb{T}, \tag{28b}$$

$$\lim_{t\to\infty} \frac{1}{T}\sum_{t=1}^{T}\mathbb{E}[D_0(\zeta,t)] \le C_0(\zeta,t), \ \forall \zeta \in \mathbb{K}, \tag{28c}$$

$$\lim_{t\to\infty} \frac{1}{T}\sum_{t=1}^{T}\mathbb{E}[D_1(\zeta,t)] \le C_1(\zeta,t), \ \forall \zeta \in \mathbb{L}. \tag{28d}$$

Constraints (25c) and (25d) in $(\mathcal{P}1)$ are, respectively, replaced by constraints (28c) and (28d) in $(\mathcal{P}2)$. (28c) requires the average WiFi user throughput loss to be kept below a limit. (28d) requires the average waste of LAA unlicensed resource to be lower than the maximum LAA padding. We observe that $(\mathcal{P}2)$ is a relaxation of $(\mathcal{P}1)$, and the optimal value denoted as $H^H_{\mathcal{P}2}$ of $(\mathcal{P}2)$ is smaller than the optimal value $H^H_{\mathcal{P}1}$ of $(\mathcal{P}1)$, i.e., $H^H_{\mathcal{P}2} \le H^H_{\mathcal{P}1}$.

We propose to solve $(\mathcal{P}2)$ by applying the Lyapunov-drift-penalty technique [30]. Under Lyapunov-drift-penalty technique, we do not require any prior information about the distribution of data arrivals and historical network states. We require only the information of current queue lengths and throughput of both LAA and WiFi users.

B. Optimization based on Lyapunov Drift Technique

To achieve fair queue stability, we first define a Lyapunov function

$$L(\boldsymbol{X}(t)) \triangleq \frac{1}{2}\left(\sum_{k=1}^{K}(X_0(k,t))^2 + \sum_{\ell=1}^{L}(X_1(k,t))^2\right), \tag{29}$$

as a sum of virtual queue length squares. Define $\boldsymbol{X}_0(t) = [X_0(1,t), \cdots, X_0(K,t)]$, $\boldsymbol{X}_1(t) = [X_1(1,t), \cdots, X_1(L,t)]$, and $\boldsymbol{X}(t) = [\boldsymbol{X}_0(t), \boldsymbol{X}_1(t)]$. The Lyapunov-drift-function becomes

$$\triangle \boldsymbol{X}(t) = \mathbb{E}[L(\boldsymbol{X}(t+1)) - L(\boldsymbol{X}(t)) \,|\boldsymbol{X}(t)]. \tag{30}$$

Thus, the Lyapunov-drift-penalty function can be defined as

$$\triangle_\nu \boldsymbol{X}(t) = \frac{\triangle \boldsymbol{X}_0(t)}{V_0} + \frac{\triangle \boldsymbol{X}_1(t)}{V_1} + \mathbb{E}\left[\sum_{\ell=1}^{L} H(\ell,t) \mid \boldsymbol{X}(t)\right], \tag{31}$$

where V_0 and V_1 are the tradeoff parameters between LAA throughput, unlicensed resource utilization, and WiFi performance loss. The upper bound of $\triangle_\nu \boldsymbol{X}(t)$ as specified in the following lemma plays a pivotal role to find the asymptotic solution of $(\mathcal{P}1)$.

Definition 1: The Lyapunov-drift-penalty of $\triangle \boldsymbol{X}(t)$ can be formulated as

$$\triangle_\nu \boldsymbol{X}(t) \leq \sum_{v=0}^{1} \frac{B_v}{V_v} + \mathbb{E}\left[\sum_{v=0}^{1}\sum_{\zeta=1}^{G(v)} \frac{X_v(\zeta,t)}{V_v}\left[C_v(\zeta,t) - D_v(\zeta,t)\right] + \sum_{\ell=1}^{L} H(\ell,t) \mid \boldsymbol{X}(t)\right], \tag{32}$$

where $G(0)=K$, $G(1)=L$, $B_0 = \frac{1}{2}\sum_{\ell=1}^{L}\left(\alpha(\ell)\right)^2$ and $B_1 = \frac{1}{2}\sum_{k=1}^{K}\left(\beta(k)\right)^2$.

Proof: See Appendix A. ∎

Note the i.i.d. decisions among (32) for different time slots. Thus, the objective function of $(\mathcal{P}2)$ can be decoupled by solving the following problem in each time slot after removing the constants $\sum_{v=0}^{1}\frac{B_v}{V_v}$ and $\sum_{v=0}^{1}\sum_{\zeta=1}^{G(v)}\frac{X_v(\zeta,t)}{V_v}C_v(\zeta,t)$ from the objective function

$$(\mathcal{P}3): \max_{\{J(t)\}} \sum_{\ell=1}^{L} H(\ell,t) - \sum_{v=0}^{1}\sum_{\zeta=1}^{G(v)} \frac{X_v(\zeta,t)}{V_v} D_v(\zeta,t), \tag{33}$$
$$\text{subject to} \quad T_1(t) = J(t)\,T_0, \quad \forall t \in \mathbb{T}.$$

$(\mathcal{P}3)$ is an integer optimization problem, which can be tackled via exhaustive enumeration. From (28d), we find that $J(t) \leq \min_{\ell}\left\{\frac{\alpha(\ell)+H(\ell,t)}{T_0}\right\}$ for $v=1$. For $v=0$, let $J_{\mathrm{T}}(k,t)$ be the maximum value to satisfy $\sum_{j=0}^{J(t)-1} R_0(k,t+j)\,\widetilde{T}_0 \leq \beta(k)$. We can see that $J(t) \leq \min_{k}\{J_{\mathrm{T}}(k,t)\}$. Then, we can narrow the search range for optimum $J^H(t)$ to $\left[1, \min\left\{\frac{\alpha(\ell)+H(\ell,t)}{T_0}, J_{\mathrm{T}}(k,t)\right\}\right]$[5]. We describe the algorithm to optimize TXOP length for LAA network in Table II.

We now show that the solution of $(\mathcal{P}3)$ is asymptotically optimum for $(\mathcal{P}1)$. According to the stationary and randomized policy in [30], [32], the optimal solution of (33) behaves arbitrarily close to that from $(\mathcal{P}2)$. There exists an arbitrarily small gap between

$$\mathbb{E}\left[\sum_{v=0}^{1}\sum_{\zeta=1}^{G(v)} D_v(\zeta,t)\right] \text{ and } \mathbb{E}\left[\sum_{v=0}^{1}\sum_{\zeta=1}^{G(v)} C_v(\zeta,t)\right].$$

Therefore, the following lemma helps define the asymptotic optimality of $(\mathcal{P}3)$.

Definition 2: Given a $\delta > 0$, there exists a stationary and randomized policy Π for $(\mathcal{P}2)$, such that the optimal solution can be described as $J^{\Pi}(t)$, for which the following inequalities

[5]The maximum transmission duration for LAA can be formulated as $J^{\max}(t) = \min\left\{\frac{\alpha(\ell)+H(\ell,t)}{T_0}, J_{\mathrm{T}}(k,t)\right\}$.

TABLE II
THE ALGORITHM OF OPTIMAL TXOP LENGTH DECISION.

Algorithm 2 The algorithm of optimal TXOP length decision.

1: **Initialize** $t=1$, $X(0)=0$, $\alpha(\ell), \forall \ell \in \mathbb{L}$, and $\beta(k), \forall k \in \mathbb{K}$.
2: **Do**
3: Obtain the virtual queue state $\boldsymbol{X}(t)$, the data rate of WiFi user $R_{0'}(k,t)$ and LAA user $R_1(\ell,t)$ from (19) and (18), respectively.
4: Exhaustively find $J^H(t)$ that determines the optimal TXOP length by solving the i.i.d. time slot problem $(\mathcal{P}3)$, i.e.,

$$J^H(t) = \arg\max \left\{\sum_{\ell=1}^{L} H(\ell,t) - \sum_{v=0}^{1}\sum_{\zeta=1}^{G(v)} \frac{X_v(\zeta,t)}{V_v} D_v(\zeta,t)\right\}, \tag{34}$$

subject to $T_1(t) = J(t)\,T_0$ and $1 \leq J(t) \leq \min\left\{\frac{\alpha(\ell)+H(\ell,t)}{T_0}, J_{\mathrm{T}}(k,t)\right\}$.
5: Update the queues according to (26) and (27).
6: Set $t = t+1$.
7: **Until** break.

hold

$$\mathbb{E}\left[\sum_{\ell=1}^{L} H^{\Pi}(\ell,t)\right] \leq H^H_{\mathcal{P}2} + \delta, \quad \forall t \in \mathbb{T}, \tag{35}$$

$$\sum_{v=0}^{1}\sum_{\zeta=1}^{G(v)} \mathbb{E}\left[\left|D_v^{\Pi}(\zeta,t) - C_v(\zeta,t)\right|\right] \leq \rho\delta, \quad \forall t \in \mathbb{T}, \tag{36}$$

where $\rho \geq 0$ is a scaling constant.

Proof: See Theorem 4.5 in [30]. ∎

The next theorem defines the asymptotic optimality of $(\mathcal{P}3)$.

Theorem 1: The optimal value for $(\mathcal{P}3)$, denoted as $H^H_{\mathcal{P}3}$, is upper bounded by the optimal value for $(\mathcal{P}1)$, denoted as $H^H_{\mathcal{P}1}$, such that

$$H^H_{\mathcal{P}3} \leq H^H_{\mathcal{P}1} + \sum_{v=0}^{1}\frac{B_v}{V_v}. \tag{37}$$

Proof: See Appendix B. ∎

From Theorem 1, the upper bound $H^H_{\mathcal{P}1} + \sum_{v=0}^{1}\frac{B_v}{V_v}$ can be made very tight by selecting asymptotically large V_0 and V_1. Hence, our Lyapunov algorithm to solve the Lyapunov problem $(\mathcal{P}3)$ can asymptotically achieve the optimum performance of the original design problem $(\mathcal{P}1)$.

VI. PERFORMANCE EVALUATION

We now present numerical results to assess the performance of the proposed coexistence mechanism. In our simulation, we assume an HAP to have 4, 6, and 8 antennas, respectively. We generate 20 LAA users and 20 WiFi users, which are uniformly distributed within the HAP coverage. The WiFi users are randomly selected to associate with the WiFi side of the HAP initially. Each selected WiFi user can occupy a stream to transmit 256 subframes in the A-MPDU at the PHY data rate of 1 Gpbs. The WiFi occupation duration and the related simulation parameters are based on [23], [31]. Moreover, WiFi and LAA users both have i.i.d. Rayleigh fading channels with zero mean and unit variance. Although

TABLE III
SYSTEM PARAMETERS

Parameters	Settings
Bandwidth	20 MHz
Iteration times (PPDU)	1000
Max. A-MPDU size	256 frames
Packet length	1500 bytes
PHY data rate	1 Gbps
RU tones	106
Bandwidth of each tone	78.125 kHz
Bandwidth of each RB	15 kHz
Number of RBs (20 MHz)	100
Number of antennas	4, 6, 8
Number of LAA and WiFi users	20, 20
Min. data rate requirement on each RU	$4 \sim 7$ Mbps
WiFi delay loss tolerance	0.78/0.85 Mbit
Max. padding length of LAA	3 ms
LAA transmission power	27 dBm/30 dBm
WiFi transmission power	25 dBm/27 dBm

the LAA and WiFi access hosts are integrated into one entity, they are still two separated and standard compliant network hosts. Moreover, LAA nodes are assumed to typically have larger coverage than WiFi nodes. Therefore, in this simulation, two sets of transmission powers for WiFi and LAA components are considered: $\boldsymbol{P_A} = \{P_0 = 25 \text{ dBm}, P_1 = 27 \text{ dBm}\}$ and $\boldsymbol{P_B} = \{P_0 = 27 \text{ dBm}, P_1 = 30 \text{ dBm}\}$. Furthermore, we select RU with 106 tones to support 8 users according to the RU allocation table in [11]. Without loss of generation, we mainly consider the performance for one RU here. System parameters are summarized in Table III.

A. Stream Selection and User Replacement

We first demonstrate the flexibility and feasibility of our proposed user selection and replacement strategy, as well as the effects of various system parameters. Here, we implement the select-and-replace process according to Algorithm I.

The relationship between the removed WiFi users and the replacement LAA users are shown in Fig. 5. In particular, Fig. 5(a) depicts the average number of removed WiFi users for different values of WiFi user rate threshold on each RU R_{T}. It is intuitive that the average number of removed WiFi users grows with larger rate threshold. Furthermore, higher WiFi transmission power under the same rate threshold would lead to fewer WiFi user removal, since higher power leads to higher data rate. Similarly, HAP with larger number of antennas would initially be able to support more WiFi users of relatively low data rate on each RU. A strict rate threshold in fact would remove more such WiFi users. To ensure the existence of WiFi users, we command at least one WiFi user should be associated with the HAP. As the WiFi rate threshold becomes too high, all the WiFi users would be removed.

At the same time, Fig. 5(b) shows the average number of new LAA user replacement under different WiFi rate thresholds on each RU. Since Fig. 5(a) shows that larger data rate threshold leads to more WiFi user removals, they would concede more spectrum resource for LAA user transmission. Therefore, the average number of replacement LAA users increases with the WiFi rate threshold. Consistent with the results of Fig. 5(a), either more antennas or lower WiFi power would allow more LAA user accommodation.

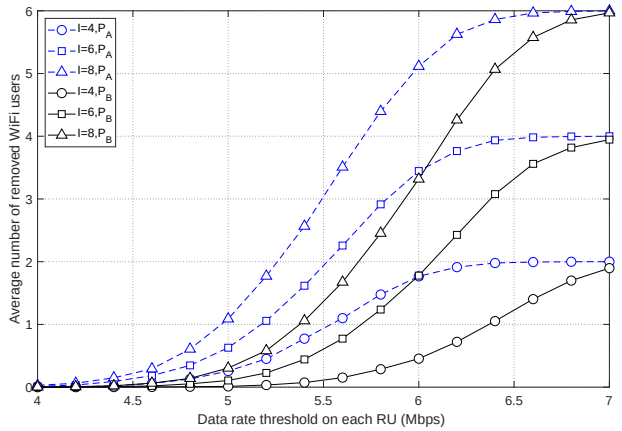

(a) Average number of removed WiFi users under different WiFi user data rate threshold on each RU.

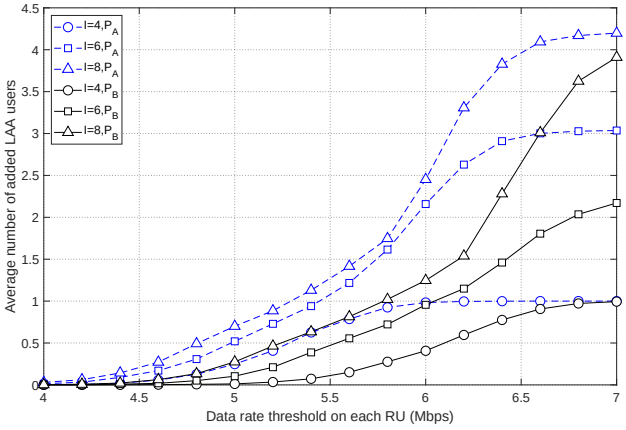

(b) Average number of added LAA users under different WiFi user data rate thresholds on each RU.

Fig. 5. Average number of removed WiFi users vs added LAA users.

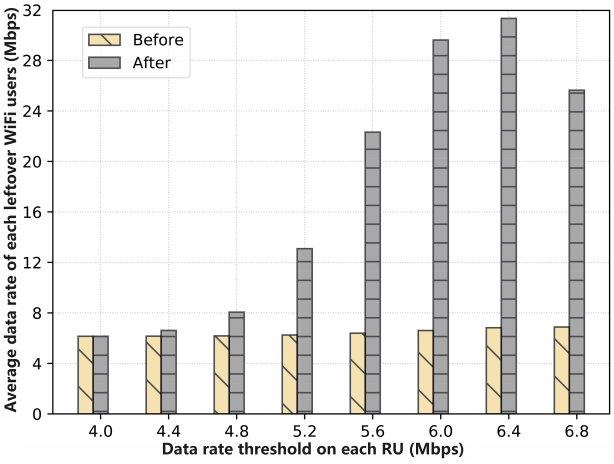

Fig. 6. Average data rate of each leftover WiFi user before and after user replacements.

Fig. 6 illustrates the average data rate of remaining WiFi users before and after user replacement under different WiFi rate threshold on each RU. According to Fig. 5(a), the number

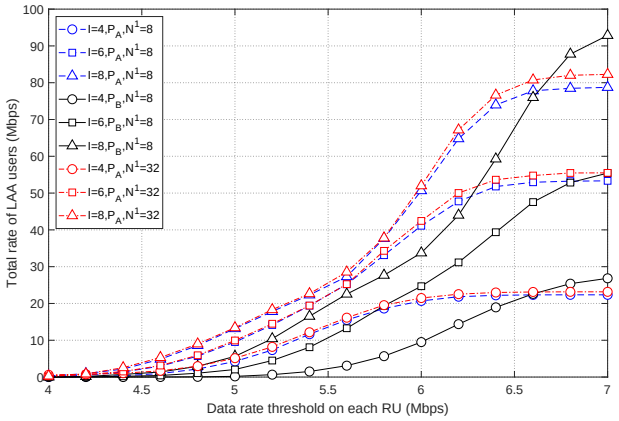

(a) Total average data rate of new added LAA users.

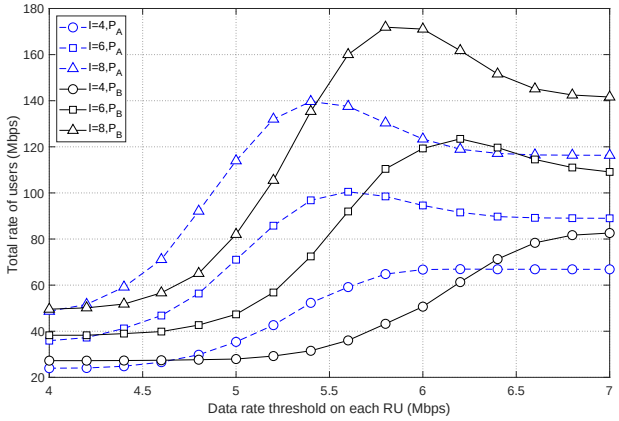

(b) Total average data rate of all the associated users.

Fig. 7. Coexistence network performance after the stream selection and user replacement strategy.

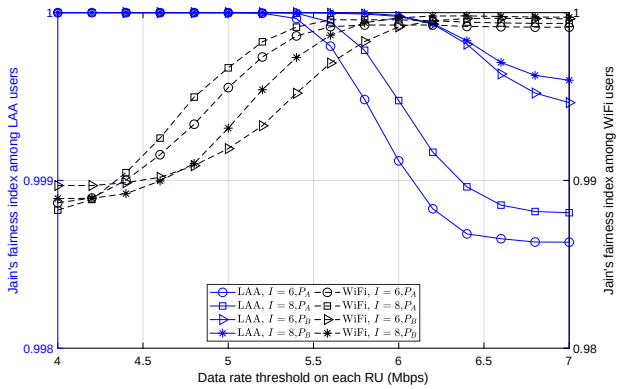

(a) The fairness among LAA/WiFi users.

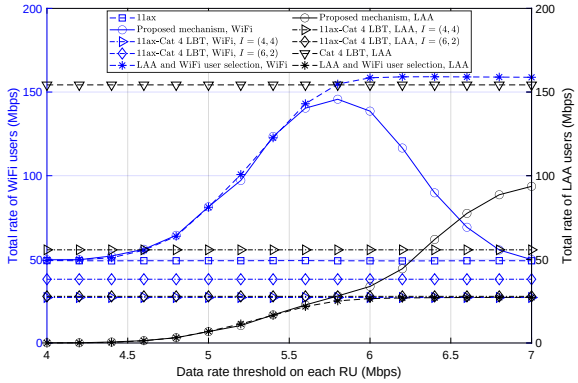

(b) Performance comparison between the proposed mechanism and the standardized mechanisms.

Fig. 8. The fairness analysis and performance comparison for the proposed mechanism.

of removed WiFi users increases with the data rate threshold. Naturally, Fig. 6 shows that the remaining WiFi users will initially achieve higher average data rate for larger rate thresholds, since poorer WiFi users are first removed and there will be less WiFi contention. However, when the data rate threshold exceeds 6.4 Mbps, poorer WiFi users have already been discarded, which means user replacement would not bring further performance enhancement. Then, the average data rate of each leftover WiFi user declines.

Fig. 7 captures a metric of coexistence network performance after the stream selection and user replacement strategy. Specifically, Fig. 7(a) shows the growth of sum LAA data rate in response to increasing WiFi data rate threshold on each RU. When the data rate threshold on each RU is small, more weaker WiFi connections have been replaced under lower transmission power. Therefore, the total LAA rate under higher transmission power would be smaller than that under lower transmission power. It is interesting to note that this growth eventually saturates after most weaker WiFi connections have been terminated and replaced, as Fig. 5(b) had shown. Thereafter, no more LAA users would be added and the total LAA rate would remain level. This figure also shows that the sum LAA data rate would increase with the number of available LAA users that may offer better replacement candidates, though the gap between $|\mathbb{N}_1| = 8$ and $|\mathbb{N}_1| = 32$ is rather negligible. In Fig. 7(b), we illustrate the total data rate of all associated LAA and WiFi connections. Corresponding to Fig. 7(a), we find the results to achieve a maximum whose location would vary with the number of antennas and power settings. Meanwhile, the total user rate would also asymptotically approach flat level.

Fig. 8(a) depicts the fairness comparison among LAA/WiFi users. Jain's fairness index is used to characterize the fairness [33], which can be defined as

$$\mathcal{J} = \frac{(\sum_k x_k)^2}{K \sum_k x_k^2}, \tag{38}$$

where $x_k = \tilde{R}_0(k), \forall k \in \mathbb{M}/\mathbb{K}$, $K = |\mathbb{M} - \mathbb{K}|$ for WiFi users, and $x_k = R_1(k), \forall k \in \mathbb{L}$, $K = |\mathbb{L}|$ for LAA users.

From this figure, either LAA users or WiFi users achieve fairness. Specifically, the LAA users can achieve better fairness than the WiFi users, since LAA users are added in an order according to their channel gains. Moreover, the fairness among LAA users improves with the antenna number and the transmit power, which presents more selection opportunities for LAA users. Meanwhile, the terminated and remaining WiFi users would also impact the fairness difference among WiFi users. As the data rate threshold increases, the number of added LAA users increases and thus the fairness decreases. On the contrary, the fairness among WiFi users increases with the data rate threshold because of the removal of WiFi users with poorer links.

Fig. 8(b) shows the performance comparison between the

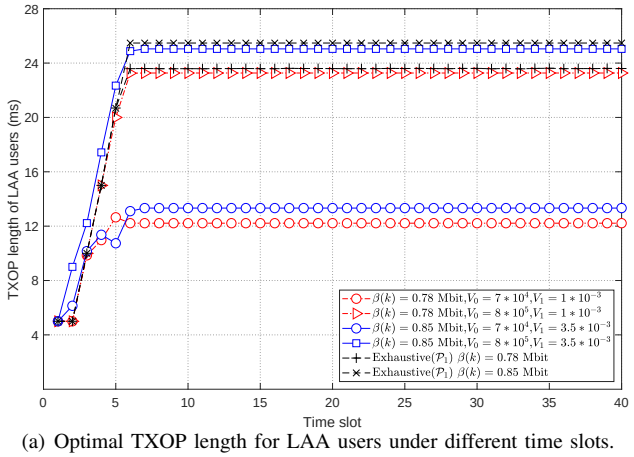

(a) Optimal TXOP length for LAA users under different time slots.

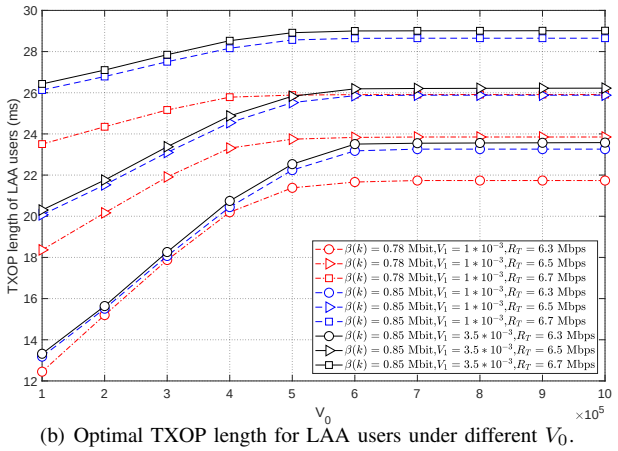

(b) Optimal TXOP length for LAA users under different V_0.

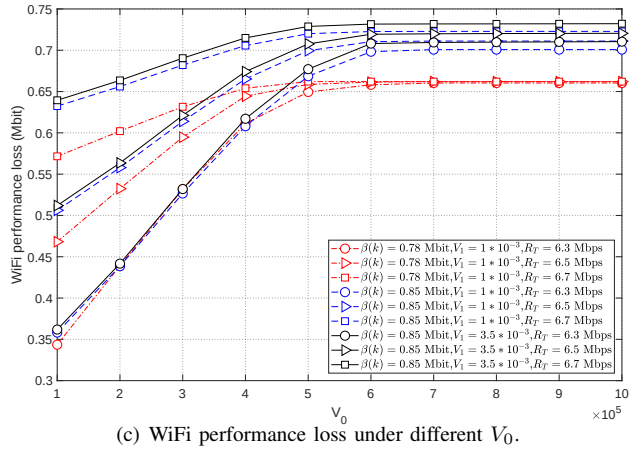

(c) WiFi performance loss under different V_0.

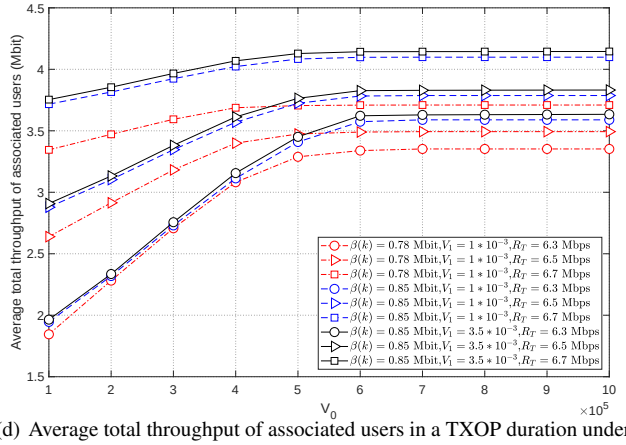

(d) Average total throughput of associated users in a TXOP duration under different V_0.

Fig. 9. Convergence property of the proposed Lyapunov optimization algorithm.

proposed access mechanism and the standardized access protocols. We adopt the Cat 4 LBT scheme in 3GPP Release 13 as the standardized LAA access protocol [24]. The WiFi mechanism with IEEE 802.11ax standard, the LAA mechanism with Cat 4 LBT scheme, and the WiFi and LAA coexistence mechanism with 11ax-Cat 4 LBT protocol are given as benchmarks. To show the results more clearly, we consider $\boldsymbol{P_B}$ as the set of transmission power. To make a fair performance comparison, we consider both the HAP, WiFi AP, and the access point for LAA mechanism each have 8 antennas. For comparability, we consider two WiFi-LAA antenna sets for the 11ax-Cat 4 LBT based coexistence mechanism, i.e., $\boldsymbol{I}=(4,4)$ and $\boldsymbol{I}=(6,2)$, each that the total antenna number remains 8. From the results in this figure, the proposed mechanism delivers the highest WiFi performance, whereas the 11ax-Cat 4 LBT mechanism has the lowest. Intuitively, the proposed mechanism utilizes a select-and-replace scheme by dropping poorer WiFi links and adding LAA users with better links to mitigate interference and to improve the performance of both LAA and WiFi networks. However, WiFi itself does not have a select-and-replace capability. Therefore, the proposed mechanism has higher WiFi performance than the WiFi mechanism. Under the 11ax-Cat 4 LBT mechanism, WiFi users have to compete with the LAA users for the unlicensed resources. Hence, the 11ax-Cat 4 LBT mechanism shows lower WiFi performance than pure WiFi. On the other aspect, as the data rate threshold of each RU increases, the LAA performance of the proposed mechanism starts below the 11ax-Cat 4 LBT mechanism before surpassing it. According to Fig. 4(b), the average number of added LAA users is quite small when the data rate threshold on each RU is less than 4.6 Mbps. With the increment of added LAA users, the advantage of the proposed new mechanism becomes apparent. Furthermore, the 11ax-Cat LBT mechanism equipped more antennas has higher performance than that under fewer antennas. In addition, the LAA mechanism shows the upper bound of LAA performance since it operates without considering the coexistence with WiFi. In this figure, we also present the case that both LAA and WiFi users participate into the user replacement strategy. Intuitively, it achieves much higher WiFi performance and lower LAA performance than the proposed mechanism since it would select WiFi users with better links instead of LAA users with poorer links.

The computational complexities of both the IEEE 802.11ax and 11ax-Cat 4 LBT based access mechanisms are linear with respect to the serviced user number. The computational complexity of the proposed access mechanism mainly comes from the select-and-replace algorithm with $\mathcal{O}\left(7/6|\mathbb{N}_1|I^3\right)$ [18]. Therefore, our proposed access mechanism is still competitive under acceptable number of antennas.

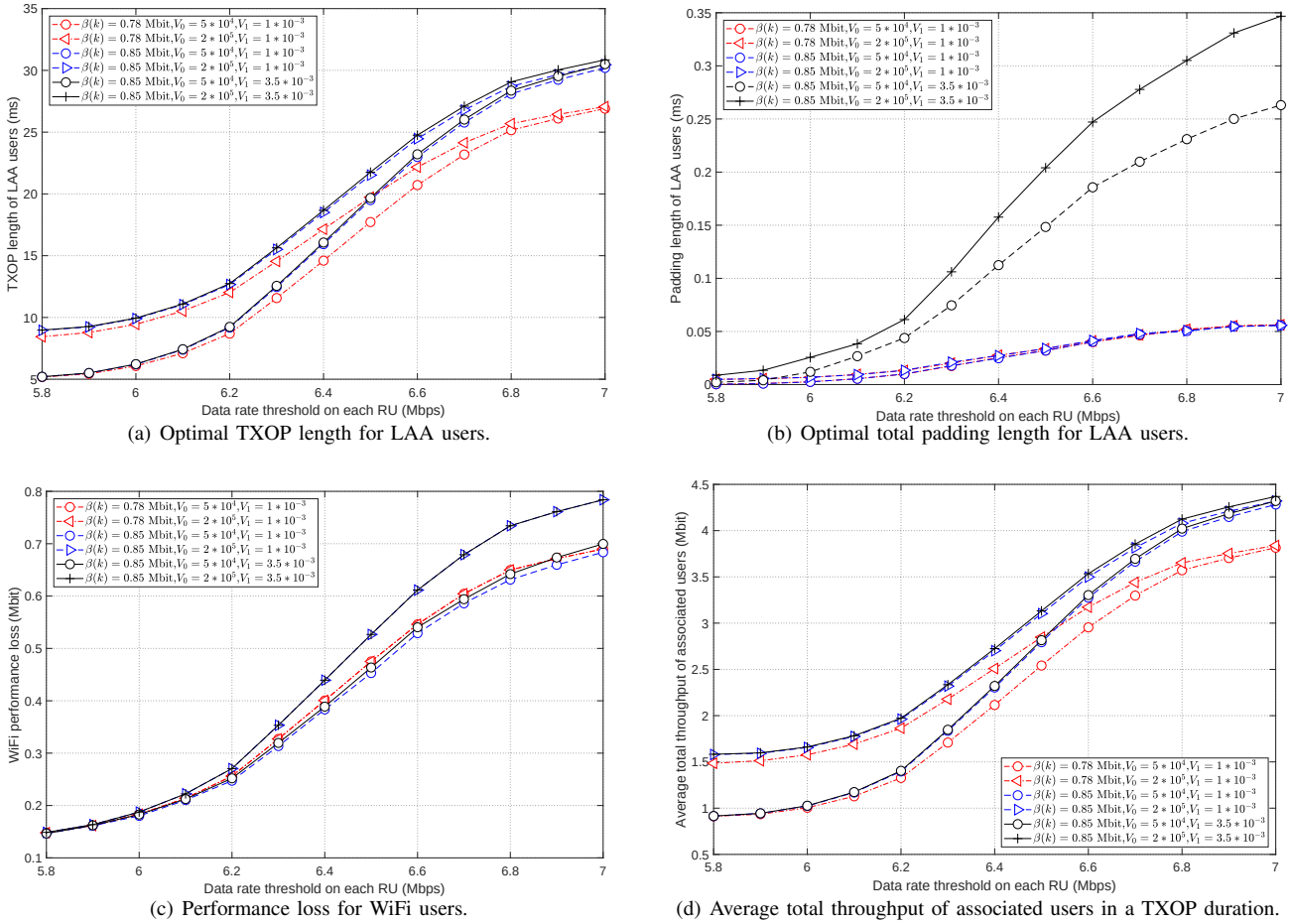

(a) Optimal TXOP length for LAA users.

(b) Optimal total padding length for LAA users.

(c) Performance loss for WiFi users.

(d) Average total throughput of associated users in a TXOP duration.

Fig. 10. Optimized TXOP, padding lengths, WiFi performance loss, and total throughput under various data rate threshold on each RU.

B. Lyapunov based TXOP Optimization

We now test the outcomes of the proposed TXOP optimization algorithm based on the Lyapunov queue function. Here, we assume that both LAA and WiFi users receive data packets of Poisson arrival. The arrival rates are set to $1.5R_1(\ell)$ for LAA user ℓ and $1.5R_0(m)$ for WiFi user m, respectively. We also set the maximum padding length for LAA user to $\alpha(\ell) = 3$ ms, $\forall \ell$. We allow WiFi users to have the same delay loss tolerance, which is set as either $\beta(k) = 0.78$ Mbit or $\beta(k) = 0.85$ Mbit, respectively.

Fig. 9 presents the convergence behavior of the proposed Lyapunov optimization solution. In Fig. 9(a), we introduce an exhaustive algorithm for $(\mathcal{P}1)$ as a performance benchmark through iteratively computing. The TXOP length of LAA users in time slot t is related to the status in the previous $t-1$ time slots. The data rate threshold on each RU is set to $R_{\mathrm{T}} = 6.3$ Mbps. From this figure, we can observe that the optimized TXOP length first grows, and eventually stabilizes after about $5-7$ time slots, which verifies the rapid convergence speed of the proposed algorithm. Moreover, it is obvious that the benchmark greedy algorithm may outperform our Lyapunov optimization algorithm. However, larger selections of V_0 and V_1 would lead to a longer TXOP length, and closer to the greedy algorithm, as Theorem 1 had established. Thus, the high efficiency of Lyapunov optimization algorithm is at the expense of some performance degradation.

Fig. 9(b), Fig. 9(c), and Fig. 9(d) show the optimized TXOP length, WiFi performance loss/throughput decrement, and total throughput under different values V_0. It is intuitive that longer TXOP length coincides with higher WiFi performance loss, and thus larger total throughput since LAA network has higher spectrum efficiency than WiFi network. Furthermore, similar to the observation from Fig. 9(a), optimized TXOP length for LAA users would increase with V_0, and saturates when V_0 is sufficiently large. From Fig. 9, we can also conclude that looser WiFi delay loss tolerance leads to higher LAA performance improvement and WiFi performance loss decrement.

In the last set of results, Fig. 10 illustrates the relationship between the optimized TXOP length $J^H(t)$ and total optimal padding length for LAA users, i.e., $\sum_\ell \left(T_1\left(t\right) - H\left(\ell, t\right)\right)$. From Fig. 10(a), $J^H(t)$ increases with increasing WiFi data threshold as LAA users can acquire more resources. The optimized TXOP length for LAA users also grows. When the WiFi data rate threshold is too large, however, almost all WiFi users have been removed. Any changes in V_0 and V_1 for LAA users would not further influence the optimized TXOP length. Together with Fig. 10(a), Fig. 10(b) illustrates the total padding length for LAA users under optimized TXOP lengths. Fig. 10(b) shows LAA users to waste more resources

for longer TXOP. The growing performance loss of WiFi users is more than offset by the growth of total throughput of all the associated users, as shown in Fig. 10(c) and Fig. 10(d). For this reason, to improve spectrum efficiency and maintain satisfactory WiFi performance, the data rate threshold should be set judiciously.

VII. Conclusion

In this paper, we propose a novel spatial multiplexing based LAA structure within the IEEE 802.11ax protocol. To provide a harmonious environment for LAA and WiFi coexistence, we develop a stream selection and user replacement strategy for MU-MIMO transmission with ZFBF. Additionally, we derive a new design methodology for TXOP optimization based on the practical online Lyapunov optimization technique, which requires little prior knowledge and possesses low complexity. Performance analysis established the asymptotic optimality of the proposed Lyapunov optimization based algorithm. Our numerical results showed that the performance of both WiFi and LAA users can be improved according to the stream selection and user replacement strategy. They further demonstrated the effectiveness of the Lyapunov optimization in resource allocation.

Appendix A: Proof of Lemma 1

Without the expectation, (30) can be rewritten as

$$\triangle \boldsymbol{X}(t) = L(\boldsymbol{X}(t+1)) - L(\boldsymbol{X}(t)). \tag{39}$$

Substituting (29) into (39) leads to

$$\triangle \boldsymbol{X}(t) = \frac{1}{2}\sum_{v=0}^{1}\sum_{\zeta=1}^{G(v)}\left[(X_v(\zeta,t+1))^2 - (X_v(\zeta,t))^2\right]. \tag{40}$$

Considering $\left([x]^+\right)^2 \le (x)^2$ in (26) and (27), we have

$$\begin{aligned}&(X_v(\zeta,t+1))^2 - (X_v(\zeta,t))^2\\ &\le 2X_v(\zeta,t)\left(C_v(\zeta,t) - D_v(\zeta,t)\right) + \left(C_v(\zeta,t) - D_v(\zeta,t)\right)^2\\ &\le 2X_v(\zeta,t)\left(C_v(\zeta,t) - D_v(\zeta,t)\right) + \left(C_v(\zeta,t)\right)^2,\end{aligned} \tag{41}$$

for $v = 0$ and $\zeta \in \mathbb{K}$; or for $v = 1$ and $\zeta \in \mathbb{L}$. Since $C_0(k,t) \le \beta(k)$ and $C_1(\ell,t) \le \alpha(\ell)$, the upper bound of (40) can be formulated as

$$\begin{aligned}\frac{\triangle \boldsymbol{X}_v(t)}{V_v} &= \frac{1}{2}\sum_{v=0}^{1}\frac{1}{V_v}\sum_{\zeta=1}^{G(v)}\left((X_v(\zeta,t+1))^2 - (X_v(\zeta,t))^2\right)\\ &\le \sum_{v=0}^{1}\frac{B_v}{V_v} + \sum_{v=0}^{1}\sum_{\zeta=1}^{G(v)}\frac{X_v(\zeta,t)}{V_v}\left(C_v(\zeta,t) - D_v(\zeta,t)\right),\end{aligned} \tag{42}$$

where $B_0 = \frac{1}{2}\sum_{\ell=1}^{L}(\alpha(\ell))^2$ and $B_1 = \frac{1}{2}\sum_{k=1}^{K}(\beta(k))^2$. Adding $\mathbb{E}\left[\sum_{\ell=1}^{L}H(\ell,t)\right]$ to both sides of (42) before taking expectation condition on $\boldsymbol{X}(t)$, we can obtain (32). This completes the proof.

Appendix B: Proof of Theorem 1

From Lemma 1, the optimal solution of $(\mathcal{P}2)$ can be asymptotically achieved by solving the per-time slot problem from Lyapunov-drift-penalty. We can further find that

$$\begin{aligned}\triangle_\nu \boldsymbol{X}(t) &= \frac{\triangle \boldsymbol{X}_0(t)}{V_0} + \frac{\triangle \boldsymbol{X}_1(t)}{V_1} + \mathbb{E}\left[\sum_{\ell=1}^{L}H(\ell,t) \mid \boldsymbol{X}(t)\right]\\ &\le \frac{\triangle \boldsymbol{X}_0(t)}{V_0} + \frac{\triangle \boldsymbol{X}_1(t)}{V_1} + H^H_{\mathcal{P}_3}\\ &\overset{(a)}{\le} \sum_{v=0}^{1}\frac{B_v}{V_v} + \mathbb{E}\left[\sum_{v=0}^{1}\sum_{\zeta=1}^{G(v)}\frac{X_v(\zeta,t)}{V_v}(t)\left(C_v(\zeta,t) - D_v^*(\zeta,t)\right)\right.\\ &\quad\left. + \sum_{\ell=1}^{L}H^H(\ell,t) \mid \boldsymbol{X}(t)\right]\\ &\le \sum_{v=0}^{1}\frac{B_v}{V_v} + \mathbb{E}\left[\sum_{v=0}^{1}\sum_{\zeta=1}^{G(v)}\frac{X_v(\zeta,t)}{V_v}(t)\left(C_v(\zeta,t) - D_v^{\Pi}(\zeta,t)\right)\right.\\ &\quad\left. + \sum_{\ell=1}^{L}H^{\Pi}(\ell,t)\right]\\ &\overset{(b)}{\le} \sum_{v=0}^{1}\frac{B_v}{V_v} + \varrho\delta\mathbb{E}\left[\sum_{v=0}^{1}\sum_{\zeta=1}^{G(v)}\frac{X_v(\zeta,t)}{V_v}(t)\right] + \left(H^H_{\mathcal{P}_2} + \delta\right),\end{aligned} \tag{43}$$

where inequalities (a) and (b) are owing to Lemma 1 and Lemma 2, respectively.

Letting $\delta \to 0$, we have

$$\begin{aligned}\sum_{v=0}^{1}\frac{\triangle \boldsymbol{X}_v(t)}{V_v} + H^H_{\mathcal{P}_3} &\le \lim_{\delta\to 0}\sum_{v=0}^{1}\frac{B_v}{V_v} + \varrho\delta\mathbb{E}\left[\sum_{v=0}^{1}\sum_{\zeta=1}^{G(v)}\frac{X_v(\zeta,t)}{V_v}\right]\\ &\quad + \left(H^H_{\mathcal{P}_2} + \delta\right)\\ &= \sum_{v=0}^{1}\frac{B_v}{V_v} + H^H_{\mathcal{P}_2}.\end{aligned} \tag{44}$$

We can further transform (44) into

$$\begin{aligned}\lim_{t\to\infty}\frac{1}{T}\sum_{t=1}^{T}\sum_{v=0}^{1}\frac{\triangle \boldsymbol{X}_v(t)}{V_v} + H^H_{\mathcal{P}_3} &\overset{(c)}{=} \lim_{t\to\infty}\frac{L(\boldsymbol{X}(T+1))}{T} + H^H_{\mathcal{P}_3}\\ &\le \sum_{v=0}^{1}\frac{B_v}{V_v} + H^H_{\mathcal{P}_2}.\end{aligned} \tag{45}$$

Here equality (c) arises from (30) as

$$\begin{aligned}L(\boldsymbol{X}(T+1)) &= \triangle \boldsymbol{X}(T) + L(\boldsymbol{X}(T))\\ &= \triangle \boldsymbol{X}(T) + \cdots + \triangle \boldsymbol{X}(1) + L(\boldsymbol{X}(0))\\ &= \sum_{t=1}^{T}\triangle \boldsymbol{X}(t).\end{aligned} \tag{46}$$

Since $\lim_{T\to\infty}\frac{L(\boldsymbol{X}(T+1))}{T} = 0$, (45) can be rewritten as

$$H^H_{\mathcal{P}_3} \le \sum_{v=0}^{1}\frac{B_v}{V_v} + H^H_{\mathcal{P}_2}. \tag{47}$$

Combining with $H^H_{\mathcal{P}2} \le H^H_{\mathcal{P}1}$ completes the proof of the theorem.

REFERENCES

[1] R. Zhang, M. Wang, L. X. Cai, Z. Zheng, X. Shen, and L. -L. Xie, "LTE unlicensed: The future of spectrum aggregation for cellular networks," *IEEE Wireless Commun.*, vol. 22, no. 3, pp. 150 - 159, Jun. 2015.

[2] B. Chen, J. Chen, Y. Gao, and J. Zhang, "Coexistence of LTE-LAA and Wi-Fi on 5 GHz with corresponding deployment scenarios: A survey," *IEEE Commun. Surveys Tuts.*, vol. 19, no. 1, pp. 7 - 32, Firstquarter 2017.

[3] A. Mukherjee, J. F. Cheng, S. Falahati, H. Koorapaty, and et al, "Licensed-assisted access LTE: coexistence with IEEE 802.11 and the evolution toward 5G," *IEEE Commun. Mag.*, vol. 54, no. 6, pp. 50 - 57, Jun. 2016.

[4] A. D. Shoaei, M. Derakhshani, and T. L. Ngoc, "Efficient LTE/Wi-Fi coexistence in unlicensed spectrum using virtual network entity: Optimization and performance analysis," *IEEE Trans. Commun.*, vol. 66, no. 6, pp. 2617 - 2629, Jun. 2018.

[5] Q. Chen, G. Yu, H. Shan, A. Maaref, G. Y. Li, and A. Huang, "Cellular meets WiFi: Traffic offloading or resource sharing?" *IEEE Trans. Wireless Commun.*, vol. 15, no. 5, pp. 3354 - 3367, May 2016.

[6] Q. Chen, G. Yu, A. Maaref, G. Y. Li, and A. Huang, "Rethinking mobile data offloading for LTE in unlicensed spectrum," *IEEE Trans. Wireless Commun.*, vol. 15, no. 7, pp. 4987 - 5000, Jul. 2016.

[7] L. Li, J. P. Seymour, L. J. Cimini, and C. C. Shen, "Coexistence of Wi-Fi and LAA networks with adaptive energy detection," *IEEE Trans. Veh. Commun.*, vol. 66, no. 11, pp. 10384 - 10393, Nov. 2017.

[8] C. Cano, D. J. Leith, A. G. Saavedra, and P. Serrano, "Fair coexistence of scheduled and random access wireless networks: Unlicensed LTE/WiFi," *IEEE/ACM Trans. Netw.*, vol. 25, no. 6, pp. 3267 - 3281, Dec. 2017.

[9] M. Hirzallah, W. Afifi, and M. Krunz, "Full-duplex-based rate/mode adaptation strategies for Wi-Fi/LTE-U coexistence: A POMDP approach," *IEEE J. Sel. Areas Commun.*, vol. 35, no. 1, pp. 20 - 29, Jan. 2017.

[10] G. J. Sutton, R. P. Liu, and Y. J. Guo, "Harmonising coexistence of machine type communications with Wi-Fi data traffic under frame-based LBT," *IEEE Trans. Commun.*, vol. 65, no. 9, pp. 4000 - 4011, Sept. 2017.

[11] IEEE. Proposed TGax draft specification. doc.: IEEE P802.11ax/D2.0, October 2017. Technical report, IEEE, 2017.

[12] E. Khorov, A. Kiryanov, A. Lyakhov, and G. Bianchi, "A tutorial on IEEE 802.11ax high efficiency WLANs," *IEEE Commun. Surveys Tuts.*, vol. 21, no. 1, pp. 197 - 216, 2018.

[13] D. J. Deng, Y. P. Lin, X. Yang, J. Zhu, Y. B. Li, J. Luo, and K. C. Chen, "IEEE 802.11ax: Highly efficient WLANs for intelligent information infrastructure," *IEEE Commun. Mag.*, vol. 55, no. 12, pp. 52 - 59, Dec. 2017.

[14] A. Ajami and H. Artail, "On the modeling and analysis of uplink and downlink IEEE 802.11ax Wi-Fi with LTE in unlicensed spectrum," *IEEE Trans. Wireless Commun.*, vol. 16, no. 9, pp. 5779 - 5795, Sept. 2017.

[15] Q. Chen, G. Yu, H. M. Elmaghraby, J. Hamalainen, and Z. Ding, "Embedding LTE-U within Wi-Fi bands for spectrum efficiency improvement," *IEEE Netw.*, vol. 31, no. 2, pp. 72 - 79, Mar. 2017.

[16] G. Geraci, A. G. Rodiguez, D. L, Perez, A. Bonfante, L. G. Giordano, and H. Claussen, "Operating massive MIMO in unlicensed bands for enhanced coexistence and spatial reuse," *IEEE J. Sel. Areas Commun.*, vol. 35, no. 6, pp. 1282 - 1293, Jun. 2017.

[17] Q. Chen, G. Yu, and Z. Ding, "Enhanced LAA for unlicensed LTE deployment based on TXOP contention," *IEEE Trans. Commun.*, vol. 67, no. 1, pp. 417 - 429, Jan. 2019.

[18] S. Huang, H. Yin, J. Wu, and V. C. M. Leung, "User selection for multiuser MIMO downlink with zero-forcing beamforming," *IEEE Trans. Veh. Commun.*, vol. 62, no. 7, pp. 3084 - 3097, Sept. 2013.

[19] M. J. Neely, "A Lyapunov optimization approach to repeated stochastic games," *online: https://arxiv.org/abs/1310.2648*, Feb. 2014.

[20] Y. Mao, J. Zhang, and K. B. Letaief, "A lyapunov optimization approach for green cellular networks with hybrid energy supplies," *IEEE J. Sel. Areas Commun.*, vol. 33, no. 12, pp. 2463 - 2477, Dec. 2015.

[21] Q. Chen, G. Yu, and Z. Ding, "Optimizing Unlicensed Spectrum Sharing for LTE-U and WiFi Network Coexistence," *IEEE J. Sel. Areas Comun.*, vol. 34, no. 10, pp. 2562-2574, 2016.

[22] R. Yin, G. Y. Li, and A. Maaref, "Spatial reuse for coexisting LTE and Wi-Fi systems in unlicensed spectrum," *IEEE Trans. Wireless Commun.*, vol. 17, no. 2, pp. 1187 - 1198, Feb. 2018.

[23] B. Boris and K. Katarzyna, "AP-initiated multi-user transmissions in IEEE 802.11ax WLANs," *online: https://arxiv.org/abs/1702.05397*, Jun. 2018.

[24] 3GPP T. 36.889, "3rd generation partnership; technical specification group radio access network; study on licensed-assisted access to unlicensed spectrum (release 13) v13.0.0.0," Jun. 2015.

[25] D. Tse and P. Viswanath, *Fundamentals of Wireless Communication.* Cambridge University Press, 2005.

[26] G. Caire and S. Shamai, "On the achievable throughput of a multiantenna Gaussian broadcast channel," *IEEE Trans. Inf. Theory*, vol. 49, no. 7, pp. 1691 - 1706, Jul. 2003.

[27] T. Yoo. and A. Goldsmith, "On the optimality of multiantenna broadcast scheduling using zero-forcing beamforming," *IEEE J. Sel. Areas Commun.*, vol. 24, no. 3, pp. 528 - 541, March 2006.

[28] M. Karaca, S. Bastani, B. E. Priyanto, M. Safavi, and B. Landfeldt, "Resource management for OFDMA based next generation 802.11 WLANs," in *Proc. IEEE WMNC*, Colmar, France, Jul. 2016, pp. 57 - 64.

[29] E. Perahia and R. Stacey, "Next generation wireless LANs: 802.11n and 802.11ac," 2nd Edition, Cambridge Press, Cambridge, 2013.

[30] M. J. Neely, *Stochastic Network Optimization with Application to Communication and Queueing Systems.* San Rafael, CA, USA: Morgan & Claypool, 2010.

[31] B. Boris and K. Katarzyna, "AP-initiated multi-user transmissions in IEEE 802.11ax WLANs," *online: https://arxiv.org/abs/1702.05397*, Jun. 2018.

[32] L. Georiadis, M. J. Neely, and L. Tassiulas, "Resource allocation and cross-layer control in wireless networks," *Foundations and Trends in Networking*, vol. 1, no. 1, pp. 1 - 149, 2006.

[33] R. Jain, D.-M. Chiu, and W. Hawe, "A quantitative measure of fairness and discrimination for resource allocation in shared computer system," Digital Equipment Corp., Hudson, MA, USA, Tech. Rep. DEC-TR-301, 1984.

Qimei Chen (S'12-M'18) received the Ph.D. degree in communication engineering from Zhejiang University, Hangzhou, China, in 2017. From 2015 to 2016, she was a Visiting Research Scholar with the School of Electrical and Computer Engineering, University of California, Davis, CA, USA. She is currently an Associate Researcher with the School of Electronic Information, Wuhan University, Wuhan, China. Her general research interests include LTE-U, WLAN, V2X, edge intelligence, and energy efficient communication techniques in next generation wireless communication systems.

Zhi Ding (S'88-M'90-SM'95-F'03) is with the Department of Electrical and Computer Engineering at the University of California, Davis, where he currently holds the position of distinguished professor. He received his Ph.D. degree in Electrical Engineering from Cornell University in 1990. From 1990 to 2000, he was a faculty member of Auburn University and later, University of Iowa. Prof. Ding has held visiting positions in Australian National University, Hong Kong University of Science and Technology, NASA Lewis Research Center and USAF Wright Laboratory. Prof. Ding has active collaboration with researchers from various universities in Australia, Canada, China, Finland, Hong Kong, Japan, Korea, Singapore, Taiwan, and USA.

Dr. Ding is a Fellow of IEEE and has been an active member of IEEE, serving on technical programs of several workshops and conferences. He was associate editor for IEEE Transactions on Signal Processing from 1994-1997, 2001-2004, and associate editor of IEEE Signal Processing Letters 2002-2005. He was a member of technical committee on Statistical Signal and Array Processing and member of technical committee on Signal Processing for Communications (1994-2003). Dr. Ding was the General Chair of the 2016 IEEE International Conference on Acoustics, Speech, and Signal Processing and the Technical Program Chair of the 2006 IEEE Globecom. He was also an IEEE *Distinguished Lecturer* (Circuits and Systems Society, 2004-06, Communications Society, 2008-09). He served on as IEEE Transactions on Wireless Communications Steering Committee Member (2007-2009) and its Chair (2009-2010). Dr. Ding is a coauthor of the text: *Modern Digital and Analog Communication Systems*, 5^{th} edition, Oxford University Press, 2019. Prof. Ding received the IEEE Communication Society's WTC Award in 2012.